PASJ: Publ. Astron. Soc. Japan **53**, 1–24, 2001 February 25

Basic Properties of Thin-Disk Oscillations [1]

Shoji KATO
Nara Sangyou University, Ikoma-gun, Nara 636-8503
kato@kusastro.kyoto-u.ac.jp

(Received 2000 September 11; accepted 2000 November 22)

Abstract

In this paper oscillations on geometrically thin disks are reviewed, focusing on two issues. One is the characteristics of disk oscillations. The other is possible excitation mechanisms of these oscillations. The main purpose of this paper is to clarify the physics and dynamics involved in these issues. We consider both Newtonian and general-relativistic disks, since a comparison of the oscillations on both disks clarifies the differences among these two oscillations and is helpful for understanding the unique properties of relativistic disks. Furthermore, we sometimes refer to stellar oscillations, since a comparison with stellar oscillations is helpful to have a deeper understanding of the disk oscillations, especially of the excitation mechanisms.

Key words: accretion, accretion disks — hydrodynamics — instabilities, viscous pulsational — oscillations, trapped, global — X-rays: stars

Contents

1. Introduction

One of the most prominent observational features of stellar black-hole candidates and AGNs is strong and chaotic time variations in X-rays. In addition, quasi-periodic oscillations (QPOs) are occasionally observed. The origins of such variabilities remain to be investigated. Some of them are suspected to be caused by an ensemble of oscillations and waves in disks. In this sense, it is worthwhile summarizing the present stage of our theoretical understanding on oscillations and waves on disks, the purpose of this paper. Concerning disk oscillations, there have been a few review articles so far (Nowak, Lehr 1998;

[1] Invited review article on a special subject.

Kato et al. 1998; Wagoner 1999). In this paper we particularly try to clarify the physics and dynamics involved in disk oscillations and their excitations.

Oscillations and waves are ubiquitous phenomena in physical systems. Accretion disks are not exceptions. Oscillations and waves on accretion disks have, however, been less studied compared with those in stars. This is partially because the existence and importance of disks in astronomical objects were recognized much later compared with stars. Disk oscillations are analogous regarding many points to stellar oscillations. There are, however, some important differences. The most prominent one comes from a difference in the force balance. Stars are nearly spherical systems, and rotation is a minor factor determining their structure. The major restoring force against small perturbations is a pressure force. In disks, on the other hand, the centrifugal force due to rotation is the major force against the gravitational force. Because of this, the major restoring force against small-amplitude perturbations superposed on disks comes from disk rotation. These differences introduce many important distinctions of disk oscillations from those of stellar ones.

The effects of the rotation on the disk oscillations are twofold. One is (i) on the characteristics of oscillation modes and the other is (ii) on the excitation mechanisms of the oscillations. In this review, we discuss these basic properties of disk oscillations, compared with those of stellar oscillations, in order to have a deeper understanding of disk oscillations.

The oscillations governed by the rotational restoring force are the inertial oscillations and their frequencies are characterized by the epicyclic frequency κ, defined by $\kappa^2 = 2\Omega(2\Omega + r d\Omega/dr)$, where Ω is the angular velocity of the disk rotation. In this sense, the radial distribution of κ is of importance in determining the behavior of oscillations. Concerning this radial distribution of κ, general relativity has important roles.

When discussing disk oscillations we should notice that disks have no definite outer boundary in the radial direction, and also the epicyclic frequency κ changes appreciably in the radial direction. Hence, for oscillations on the disks to be observable from the outside, they must be trapped in a particular region or have global patterns. One of our purposes in this paper is to examine the characteristics of oscillations satisfying such conditions. Concerning this problem, general relativity again has important roles. After discussing the dispersion relation and its characteristics in section 2, we discuss the main effects of general relativity on the dispersion relation in section 3. Sections 4 and 5 are then devoted to global oscillations and trapped ones, respectively.

Another issue to be emphasized in relation to the effects of disk rotation on oscillations is the excitation mechanism of disk oscillations. The excitation mechanisms of stellar oscillations have been well studied and are understood (e.g., Cox 1980; Unno et al. 1989). In disk oscillations, however, excitation processes which have not been considered in stellar oscillations become important in addition to those in stellar oscillations. They are viscous processes. The importance of viscous processes on excitation comes from the facts that (1) viscous heating is the major source of the heating of the disk gas and (2) the azimuthal force due to viscosity is the major source of angular-momentum transport in the radial direction. Related to these two facts, viscosity has two important processes on excitation of oscillations. One is a thermal process, and the other is a dynamical one. General relativity again acts so as to help the above processes. These issues are discussed in sections 6 and 7.

Section 8 is devoted to some issues which are not discussed in the main part of this paper, and finally a brief summary is given in section 9.

Finally, it is noted that disk-like systems are not accretion disks alone. Spiral galaxies are also disk-like systems, and their oscillations have been studied extensively after Lin and Shu (1964). Some of knowledge obtained by these studies are helpful for understanding accretion-disk oscillations and instabilities, especially the dynamical properties of accretion disks. Oscillations of disk-like galaxies are, however, different from those of accretion disks, since the former are collisionless and selfgravitating, while the latter are collisional and non-selfgravitating (except for the outer regions of disks surrounding massive central objects).

2. Dispersion Relation and Its Characteristics

2.1. *Basic Equations*

We consider here the adiabatic and inviscid motions on non-selfgravitating geometrically thin disks. In order to describe the motions, we introduce cylindrical coordinates (r, φ, z) whose origin is at the center of the central object, the z-axis being taken in the direction of the disk rotation. The r-, φ-, and z-components of the velocity are denoted by v_r, v_φ, and v_z, respectively. The equation of continuity is then

$$\frac{\partial \rho}{\partial t} + \frac{\partial}{r\partial r}(r\rho v_r) + \frac{\partial}{r\partial \varphi}(\rho v_\varphi) + \frac{\partial}{\partial z}(\rho v_z) = 0, \tag{1}$$

where ρ is the density.

The r-, φ-, and z-components of the equation of motion are written, respectively, as

$$\frac{dv_r}{dt} - \frac{v_\varphi^2}{r} = -\frac{\partial \psi}{\partial r} - \frac{1}{\rho}\frac{\partial p}{\partial r}, \tag{2}$$

$$\frac{dv_\varphi}{dt} + \frac{v_r v_\varphi}{r} = -\frac{1}{\rho}\frac{\partial p}{r\partial \varphi}, \tag{3}$$

$$\frac{dv_z}{dt} = -\frac{\partial \psi}{\partial z} - \frac{1}{\rho}\frac{\partial p}{\partial z}, \tag{4}$$

where the operator d/dt is defined by

$$\frac{d}{dt} = \frac{\partial}{\partial t} + v_r\frac{\partial}{\partial r} + v_\varphi\frac{\partial}{r\partial \varphi} + v_z\frac{\partial}{\partial z}, \tag{5}$$

and ψ is the gravitational potential due to the central object, and p is the pressure. In non-selfgravitating disks, the potential, $-\psi$, is determined by the central object alone, and it is assumed here to be axisymmetric. Hence, the term $-\partial\psi/r\partial\varphi$ on the right-hand side of equation (3) has been neglected.

For inviscid adiabatic motions, the equation of energy is written as

$$\frac{dp}{dt} - \gamma\frac{p}{\rho}\frac{d\rho}{dt} = 0, \tag{6}$$

where γ is the ratio of the specific heats.

On unperturbed accretion disks there are generally large-scale convections as well as accretion flows. We neglect, however, their effects on oscillations in this article. That is, we take $(v_r, v_\varphi, v_z) = (0, r\Omega, 0)$ for unperturbed disks, where Ω is the angular velocity of disk rotation. Furthermore, Ω is taken to be approximately a function of r alone; i.e., $\Omega = \Omega(r)$. (This holds exactly when the disk gas is inviscid and barotropic, since in this case a combination of the r- and z-components of the equation of motion requires $\partial\Omega/\partial z = 0$.)

2.2. *Basic Equations for Perturbations*

On the unperturbed disks described above, small-amplitude, inviscid, and adiabatic perturbations are superposed. We consider, furthermore, particular modes of perturbations which vary as $\exp[i(\omega t - m\varphi)]$, where ω is the frequency of the perturbations and $m(= 0, 1, 2, ...)$ denotes the number of arms in the azimuthal direction.

The velocity induced by the perturbations over pure rotation is denoted by (u_r, u_φ, u_z). The density perturbations over the unperturbed density $\rho_0(r, z)$ is denoted by ρ_1. The equation of continuity describing small-amplitude perturbations is then

$$i\tilde{\omega}\rho_1 + \frac{\partial}{r\partial r}(r\rho_0 u_r) - i\frac{m}{r}\rho_0 u_\varphi + \frac{\partial}{\partial z}(\rho_0 u_z) = 0, \tag{7}$$

where

$$\tilde{\omega} = \omega - m\Omega. \tag{8}$$

Retaining only the linear parts with respect to the perturbations, we write the r-, φ-, and z- components of the equations of motion as

$$i\tilde{\omega}u_r - 2\Omega u_\varphi = -\frac{1}{\rho_0}\frac{\partial p_1}{\partial r} + \frac{\rho_1}{\rho_0^2}\frac{\partial p_0}{\partial r}, \tag{9}$$

$$i\tilde{\omega}u_\varphi + \frac{\kappa^2}{2\Omega}u_r = i\frac{m}{r\rho_0}p_1, \tag{10}$$

$$i\tilde{\omega}u_z = -\frac{1}{\rho_0}\frac{\partial p_1}{\partial z} + \frac{\rho_1}{\rho_0^2}\frac{\partial p_0}{\partial z}, \tag{11}$$

where p_1 is an Eulerian perturbation of the pressure over the unperturbed one, $p_0(r, z)$, and $\kappa(r)$ is the epicyclic frequency, defined by

$$\kappa^2 = 2\Omega\left(2\Omega + r\frac{d\Omega}{dr}\right). \tag{12}$$

The energy equation for adiabatic perturbations is written as

$$i\tilde{\omega}(p_1 - c_s^2\rho_1) = \gamma p_0(\boldsymbol{u}\cdot\boldsymbol{A}), \tag{13}$$

where c_s is the sound speed, defined by $c_s^2 = \gamma p_0/\rho_0$, and $\boldsymbol{A}$ is the Schwarzschild discriminant vector, defined by

$$\boldsymbol{A} \equiv \ln\nabla\rho_0 - \frac{1}{\gamma}\nabla\ln p_0 = \nabla\left(\ln\frac{\rho_0}{p_0^{1/\gamma}}\right). \tag{14}$$

Let us introduce the effective gravitational acceleration $\boldsymbol{g}_{\rm eff}$, defined by

$$\boldsymbol{g}_{\rm eff} \equiv \boldsymbol{g} + r\Omega^2\boldsymbol{i}_r = [-(g_{\rm eff})_r, 0, -(g_{\rm eff})_z] = \frac{1}{\rho_0}\nabla p_0, \tag{15}$$

where $\boldsymbol{i}_r$ is the unit vector in the radial direction. We further introduce N_r and N_z, defined by

$$N_r^2 = -(g_{\rm eff})_r A_r \qquad \text{and} \qquad N_z^2 = -(g_{\rm eff})_z A_z. \tag{16}$$

When $N_z^2 > 0$, for example, the entropy is stratified in the vertical direction so that the medium is convectively stable ($A_z < 0$). The quantity N_z is a measure of the frequency of gravity oscillations in the vertical direction, and is called the Brunt–Väisälä frequency in the vertical oscillations. If $N_z^2 < 0$, on the other hand, the medium is convectively unstable in the vertical direction. A similar argument can be made concerning the radial direction by N_r^2.

We introduce here h_1, defined by

$$h_1 = \frac{p_1}{\rho_0}. \tag{17}$$

The right-hand side of the equation of motions, $-(1/\rho_0)\nabla p_1 + (\rho_1/\rho_0^2)\nabla p_0$, is then written as

$$-(\boldsymbol{A} + \nabla)h_1 + \frac{i}{\tilde{\omega}}\boldsymbol{g}_{\rm eff}(\boldsymbol{u}\cdot\boldsymbol{A}). \tag{18}$$

In thin disks the absolute value of A_r is much smaller than A_z. Then, further neglecting the buoyancy force in the radial direction compared with that in the vertical direction, we write the equations of motion, (9)–(11), as

$$i\tilde{\omega}u_r - 2\Omega u_\varphi = -\frac{\partial h_1}{\partial r}, \tag{19}$$

$$i\tilde{\omega}u_\varphi + \frac{\kappa^2}{2\Omega}u_r = i\frac{m}{r}h_1, \tag{20}$$

and

$$i\tilde{\omega}u_z = -\left(A_z + \frac{\partial}{\partial z}\right)h_1 + \frac{i}{\tilde{\omega}}N_z^2 u_z. \tag{21}$$

Finally, the energy equation (13) is approximated as

$$\frac{\rho_1}{\rho_0} = \frac{1}{c_s^2}h_1 - \frac{A_z}{i\tilde{\omega}}u_z. \tag{22}$$

Equations (7), (19)–(22) are five equations for five variables: u_r, u_φ, u_z, ρ_1, and h_1.

2.3. *Derivation of the Dispersion Relation*

Eliminating u_φ from equations (19) and (20), we have

$$\frac{\partial h_1}{\partial r} - \frac{2m\Omega}{\tilde{\omega}r}h_1 = \frac{\tilde{\omega}^2 - \kappa^2}{i\tilde{\omega}}u_r. \tag{23}$$

Another relation between h_1 and u_r is obtained by eliminating ρ_1, u_φ, and u_z from equations (7), (20), (21), and (22), which is

$$\begin{aligned}&\frac{\partial}{\rho_0\partial z}\left[\frac{\rho_0}{\tilde{\omega}^2 - N_z^2}\left(A_z + \frac{\partial}{\partial z}\right)h_1\right] - \frac{A_z}{\tilde{\omega}^2 - N_z^2}\left(A_z + \frac{\partial}{\partial z}\right)h_1\\ &+\frac{1}{i\tilde{\omega}}\frac{\partial}{r\rho_0\partial r}(r\rho_0 u_r) - i\frac{m\kappa^2}{2r\Omega\tilde{\omega}^2}u_r + \left(\frac{1}{c_s^2} - \frac{m^2}{r^2\tilde{\omega}^2}\right)h_1\\ &= 0.\end{aligned} \tag{24}$$

Elimination of u_r from equations (23) and (24) gives a partial differential equation of h_1:

$$\begin{aligned}&\frac{\partial}{\rho_0\partial z}\left(\frac{\rho_0}{\tilde{\omega}^2 - N_z^2}\frac{\partial h_1}{\partial z}\right) + \frac{\partial}{\rho_0\partial z}\left(\frac{\rho_0}{\tilde{\omega}^2 - N_z^2}A_z\right)h_1\\ &-\frac{A_z^2}{\tilde{\omega}^2 - N_z^2}h_1 + \frac{\partial}{r\rho_0\partial r}\left(\frac{r\rho_0}{\tilde{\omega}^2 - \kappa^2}\frac{\partial h_1}{\partial r}\right)\end{aligned}$$

$$-\frac{2m}{\tilde{\omega}r\rho_0}\frac{\partial}{\partial r}\left(\frac{\rho_0\Omega}{\tilde{\omega}^2-\kappa^2}\right)h_1+\left[\frac{1}{c_s^2}-\frac{m^2}{r^2(\tilde{\omega}^2-\kappa^2)}\right]h_1=0. \quad (25)$$

In order to solve approximately this partial differential equation for h_1, we decompose the equation into two separated equations under some approximations, as did Nowak and Wagoner (1992, 1993). To do so, we first neglect the term $m^2/[r^2(\tilde{\omega}^2-\kappa^2)]$ compared with $1/c_s^2$, since the disk has been assumed to be geometrically thin. Next, we introduce the WKB approximation, where the radial wavelength of the perturbations is taken to be smaller than the scale length of the radial variations of the equilibrium properties of the disk. Equation (25) is then reduced to

$$\frac{\partial}{\rho_0\partial z}\left(\frac{\rho_0}{\tilde{\omega}^2-N_z^2}\frac{\partial h_1}{\partial z}\right)+\frac{\partial}{\rho_0\partial z}\left(\frac{\rho_0}{\tilde{\omega}^2-N_z^2}A_z\right)h_1$$
$$-\frac{A_z^2}{\tilde{\omega}^2-N_z^2}h_1+\frac{\partial}{\partial r}\left(\frac{1}{\tilde{\omega}^2-\kappa^2}\frac{\partial h_1}{\partial r}\right)+\frac{h_1}{c_s^2}=0. \quad (26)$$

For simplicity, we introduce here an approximation that the unperturbed disk is vertically isothermal, and thus the density is distributed in the vertical direction as

$$\rho_0(r,z)=\rho_{00}(r)\exp\left(-\frac{z^2}{2H^2}\right), \quad (27)$$

where the half-thickness of the disk, H, is related to $\Omega_K(r)$ by

$$\Omega_K^2(r)H^2(r)=\frac{p_0}{\rho_0}. \quad (28)$$

A dimensionless vertical coordinate η is introduced by using the half-thickness of the disks, $H(r)$, as $\eta = z/H(r)$. Equation (26) is now separable into r and $\eta \equiv z/H(r)$ to the lowest WKB order; that is, by setting $h_1 = h_1^*(r)g(r,\eta)$ with g a slowly-varying function of r, we can approximate equation (26) as

$$\left[\frac{\partial}{\rho_0 g\partial\eta}\left(\frac{\rho_0}{\tilde{\omega}^2-N_z^2}\frac{\partial g}{\partial\eta}\right)+\frac{H}{\rho_0}\frac{\partial}{\partial\eta}\left(\frac{\rho_0}{\tilde{\omega}^2-N_z^2}A_z\right)\right.$$
$$\left.-\frac{A_z^2}{\tilde{\omega}^2-N_z^2}\right]+\left[\frac{H^2}{h_1^*}\frac{\partial}{\partial r}\left(\frac{1}{\tilde{\omega}^2-\kappa^2}\frac{\partial h_1^*}{\partial r}\right)+\frac{H^2}{c_s^2}\right]=0. \quad (29)$$

The terms in the first large brackets are functions of η and depend only weakly on r, while the terms in the second large brackets are functions of r. Hence, we write the first brackets as $-K(r)/\tilde{\omega}^2$, and the second one as $K(r)/\tilde{\omega}^2$, where $K(r)$ is a slowly-varying function of r and is determined later by solving the separated equations with boundary conditions. By this separation we have

$$c_s^2\frac{d}{dr}\left(\frac{1}{\tilde{\omega}^2-\kappa^2}\frac{dh_1^*}{dr}\right)+\left(1-\frac{Kc_s^2}{\tilde{\omega}^2H^2}\right)h_1^*=0 \quad (30)$$

and

$$\frac{\partial}{\rho_0\partial\eta}\left(\frac{\rho_0}{\tilde{\omega}^2-N_z^2}\frac{\partial g}{\partial\eta}\right)+\frac{1}{p_0^{1/\gamma}}\frac{\partial}{\partial\eta}\left(p_0^{1/\gamma}\frac{A_zH}{\tilde{\omega}^2-N_z^2}\right)g+\frac{K}{\tilde{\omega}^2}g$$
$$=0. \quad (31)$$

The above set of the separated equations was obtained by Nowak and Wagoner (1992). They also derived the corresponding equations in the case of polytropic gases. A further generalization to cases of the general relativistic disks has been made by Perez et al. (1997). Hereafter, the asterisk attached to h_1 is neglected for simplicity without any confusion.

The above set of equations, (30) and (31), should be solved with relevant boundary conditions. We are satisfied here only with considering an idealized case. That is, the disk is convectively neutral in the vertical direction, i.e., $N_z^2 = 0$ and $A_z = 0$. This also implies that we should take $\gamma = 1$, since we are considering here vertically isothermal disks. Equation (31) is then reduced to

$$\frac{d^2g}{d\eta^2}-\eta\frac{dg}{d\eta}+Kg=0. \quad (32)$$

This is nothing but the Hermite equation. A relevant boundary condition on the surface ($\eta = \infty$) imposes that K must be zero or a positive integer (Okazaki et al. 1987), which is denoted as n. Then, $g(\eta)$ is given by the Hermite polynomials:

$$g(\eta)=H_n(\eta) \quad (n=1,2,3,\ldots). \quad (33)$$

The mode of $n = 0$ is the fundamental one in the vertical direction and g has no node in the vertical direction, while $n = 1$ is the first overtone: g ($\propto \eta$) has one node in the vertical direction, just on the equator (odd mode). Higher overtones are represented by n larger than unity.

For local perturbations whose radial wavelength is k_r, equation (30) is reduced for $\gamma = 1$ to the dispersion relation:

$$(\tilde{\omega}^2-\kappa^2)(\tilde{\omega}^2-n\Omega_K^2)=\tilde{\omega}^2c_s^2k_r^2. \quad (34)$$

This approximate form of the dispersion relation for disk oscillations was first derived by Okazaki et al. (1987). We discuss mainly this dispersion relation hereafter, since the basic properties of disk oscillations are contained in this simple approximate dispersion relation. See Nowak and Wagoner (1992), Ipser (1994), Perez et al. (1997), and Silbergleit et al. (2000) concerning the dispersion relations in more general situations.

2.4. *Coupling between Radial and Vertical Oscillations and the Classification of Oscillations*

The meaning of the dispersion relation (34) is discussed by considering some limiting cases. In the case when the oscillations have no node in the vertical direction, i.e., $n = 0$, the dispersion relation is reduced to

$$\tilde{\omega}^2=\kappa^2+k_r^2c_s^2 \qquad \text{and} \qquad \tilde{\omega}^2=0. \quad (35)$$

The former is nothing but the inertial–acoustic waves well-known in galactic dynamics. The latter is a trivial mode when $n = 0$.

Unless the specific angular momentum decreases outwards, a fluid element which is displaced in the radial direction returns to its original radius due to a restoring force resulting from the rotation. The oscillations resulting from this restoring force are called inertial oscillations, and their frequency is the epicyclic frequency $\kappa(r)$. In compressible fluids there is an additional restoring force resulting from a pressure variation, leading to acoustic oscillations. The combination of the above two restoring force brings about the above-mentioned inertial–acoustic waves.

In the long-wavelength limit in the radial direction, i.e., $k_r = 0$, on the other hand, the dispersion relation (34) is reduced to, when $n \neq 0$,

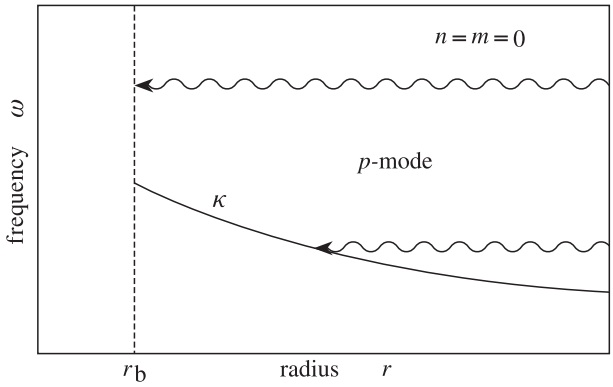

Fig. 1. Schematic diagram showing the radial region where waves of axisymmetric fundamental mode ($m = 0$, $n = 0$) can propagate on Newtonian disks. The epicyclic frequency increases inward monotonically. The radius r_b represents the radius of the surface of the central object. Near to the surface there will be a boundary layer where the disk rotation is adjusted to that of the central object. Hence, the Keplerian rotation does not represent real situations near to the boundary.

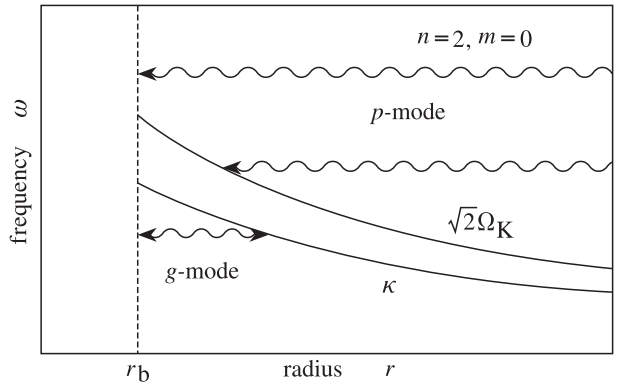

Fig. 2. Schematic diagram showing the radial regions where waves of axisymmetric $n = 2$ waves can propagate on Newtonian disks. The g-mode oscillations are trapped in an inner region of the disks.

$$\tilde{\omega}^2 = \kappa^2 \qquad \text{and} \qquad \tilde{\omega}^2 = n\Omega_K^2. \tag{36}$$

The former solution, $\tilde{\omega}^2 = \kappa^2$, represents again the inertial oscillations, while the latter represents an additional mode of oscillations. The latter is the vertical oscillation of the disks, and is related to the geometry of the disks, themselves. If a part of the disk plane is perturbed in the vertical direction, a restoring force (i.e., the vertical component of the gravitational force) acts so as to restore the perturbed part toward the equatorial plane. This brings about disk oscillations in the vertical direction. The restoring force towards the equatorial plane is $(GM/r^2)(z/r)$, which is $\Omega_K^2 z$. This means that the disks undergo harmonic oscillations around the equatorial plane and the frequency of this oscillations is Ω_K. This oscillation corresponds to the $n = 1$ mode, and is well known in galactic dynamics. This is similar to surface gravity waves which occur at the interface between two distinct fluids. If there are nodes in the vertical direction, i.e., $n \geq 2$, the frequency of the oscillations becomes higher, since the pressure restoring force is added to the above gravitational restoring force.

In the above idealized case, i.e., $k_r = 0$, horizontal oscillations ($\tilde{\omega}^2 = \kappa^2$) and vertical oscillations ($\tilde{\omega}^2 = n\Omega_K^2$) are separated. In real disks, however, both oscillations are coupled, since the disks are not homogeneous in the radial direction. That is, the oscillations on the equatorial plane with finite wavelength in the radial direction inevitably induce vertical motions because of a radial inhomogeneity of the disks. Similarly, vertical oscillations induce radial motions. Therefore, coupling between the radial and vertical oscillations inevitably occurs. Since the coupling occurs through the pressure restoring force, it is stronger when the radial wavelength is shorter and the acoustic speed is faster. Hence, the form of the dispersion relation (34) is conceivable.

The dispersion relation (34) gives two $\tilde{\omega}^2$'s for a given positive k_r^2, say $\tilde{\omega}_1$ and $\tilde{\omega}_2$ with $0 < \tilde{\omega}_1^2 < \tilde{\omega}_2^2$. The modes with higher $\tilde{\omega}^2$ (i.e., $\tilde{\omega}_2^2$) are called p-modes, while those with lower $\tilde{\omega}^2$ (i.e., $\tilde{\omega}_1^2$) are called g-modes.

In order to clarify the characteristics of axisymmetric wave modes ($m = 0$), their propagation regions on the ω–(r/r_g) plane are shown in figures 1 and 2. Figure 1 is for the fundamental modes of $n = 0$, taking ω to be positive. For waves of $m = n = 0$, we have $\omega^2 = \kappa^2 + c_s^2 k_r^2$, i.e., $\omega > \kappa$. That is, the propagation region is above the curve of $\kappa(r)$. Here, we assume that the disk touches the central object at radius r_b. If $\omega > \kappa(r_b)$, the waves can reach near to the surface of the central object, while they are reflected back outward by the barrier of the rotation when $\omega < \kappa(r_b)$ (see figure 1). In the case of $m = 0$ and $n = 1$, the detailed structure of the propagation region is delicate, since κ^2 and Ω_K^2 are close to each other in Newtonian disks. Hence, to demonstrate an example where the propagation regions are separated, we draw the case for $n = 2$ in figure 2. Since $\kappa^2 < n\Omega_K^2$ ($n = 2$), the propagation regions are bounded above and below, respectively, by two curves of κ and $2^{1/2}\Omega_K$. The region below $\kappa(r)$ is for the g-mode and the region above $2^{1/2}\Omega_K$ is for the p-mode. The propagation diagrams in the case of relativistic disks are discussed in section 5.

The terminology of the p-modes and g-modes might be somewhat confusing and misleading, since in the field of stellar oscillations the naming of the gravity mode is used for oscillations resulting from entropy stratification with $N^2 > 0$, i.e., for internal-gravity waves. The mode vanishes when $N^2 = 0$, and becomes convection when $N^2 < 0$. In deriving the dispersion relation (34) we assumed $N_z^2 = N_r^2 = 0$ from the beginning. Hence, no internal-gravity modes nor convection modes are involved in dispersion relation (34). In the case of $n = 1$, the higher frequency mode with $\tilde{\omega}_2$ is similar to the surface-gravity wave, as mentioned above, but belongs to the p-mode oscillations in our present terminology. The reason why we adopt this terminology is twofold: the first is that this classification is widely used; the second is that the behavior of the g-modes is strongly affected by the presence of a non-zero N_z, although that of the p-modes is less affected. See, for example, Kato et al. (1998) for examination of the effects of entropy stratification on the g-mode oscillations.

The first overtone ($n = 1$) (in the vertical direction) of the one-armed ($m = 1$) inertial–acoustic modes has a particular position compared with other modes. The origin of this oscillation modes is not the pressure-restoring force nor the inertial

force, unlike the other inertial–acoustic modes. This mode exists even when there is no pressure (i.e., infinitely thin disks). Rather, the characteristics of this mode becomes clear in this limiting case of no pressure. This oscillation ($n = 1$) is a vertical displacement of the disk plane with a finite wavelength in the radial direction. The restoring force of these oscillations is the gravitational force acting so as to return a fluid element to the original equatorial plane. Here, we call the mode *corrugation waves*.

Finally, an analogy between the dispersion relation (34) and that of stellar non-radial oscillations is mentioned. The latter one in the lowest WKB approximations is given by (e.g., Unno et al. 1989)

$$(\tilde{\omega}^2 - N^2)(\tilde{\omega}^2 - L_\ell^2) = \tilde{\omega}^2 c_s^2 k^2, \tag{37}$$

where N^2 is the square of the Brunt–Väisälä frequency in the radial direction [the spherical coordinates (r, θ, ϕ) centered at the stellar center are employed], k is the wavenumber in the radial direction, and L_ℓ is the Lamb frequency, defined by

$$L_\ell = \frac{\ell(\ell+1)}{r^2} c_s^2. \tag{38}$$

Here, ℓ is the degree of the spherical surface harmonic $Y_\ell^m(\theta, \phi)$ when the perturbations proportional to $Y_\ell^m(\theta, \phi)$ are considered. The Lamb waves are vertically evanescent, but horizontally propagating, acoustic waves.

As shown in equations (34) and (37), in oscillations in both disks and stars, the coupling between the radial motions and those perpendicular to them occurs through the finiteness of the radial wavelength ($k_r \neq 0$ or $k \neq 0$). In the case of disks, the radial direction is on the equatorial plane, while it is in the vertical direction to the equi-potential surface of stars in the case of stars. Accordingly, the counterpart of κ^2 in stellar oscillations is N^2 and the counterpart of $n\Omega_K^2$ in stellar oscillations is L_ℓ^2.

Nowak and Wagoner (1992) (see also Perez et al. 1997; Nowak, Lehr 1998) noticed that the differential equations describing disk oscillations are analogous to those of atmospheric oscillations (Hines 1960). The analogy between the dispersion relation of atmospheric oscillations and that of disk oscillations seems, however, to be less close , compared with the analogy between the dispersion relations of stellar oscillations (37) and disk oscillations (34).

3. Effects of General Relativity on the Dispersion Relation

The next problem is to examine how the characteristics of wave motions described by the dispersion relation (34) are modified when the effects of general relativity are taken into account. A full discussion on the dispersion relation in general-relativistic disks has been made by Ipser (1994, 1996), Perez et al. (1997) and Silbergleit et al. (2000). Here, we are satisfied with pointing out some basic modifications of the dispersion relation due to general relativity.

(a) Epicyclic Frequency κ

As mentioned before, the epicyclic frequency is an important quantity for characterizing disk oscillations. In relativistic disks, the radial distribution of the epicyclic frequency is strongly modified, as can be easily understood from the fact that it vanishes at the marginally stable radius r_{ms}. That is, the radial distribution of the epicyclic frequency is not monotonic, unlike that in Newtonian one. It increases inward in the outer non-relativistic region as does Ω_K, but after arriving at the maximum at a certain radius it decreases inward toward r_{ms}, where it vanishes. This distribution of $\kappa(r)$ is of importance in relation to the wave trapping (see Kato, Fukue 1980 for the p-mode; Okazaki et al. 1987, Nowak, Wagoner 1992, and Perez et al. 1997 for the g-mode), which will be discussed later.

The radial distribution of $\kappa(r)$ in the Kerr metric is given by (Okazaki et al. 1987)

$$\kappa^2 = \frac{GM}{r^3}\left(1 + \frac{a}{\hat{r}^{3/2}}\right)^{-2}\left(1 - \frac{6}{\hat{r}} + \frac{8a}{\hat{r}^{3/2}} - \frac{3a^2}{\hat{r}^2}\right), \tag{39}$$

where a is a dimensionless angular momentum parameter, defined by $a = cJ/(GM^2)$, J being the angular momentum of the central object, and $\hat{r}$ is a dimensionless radius defined by

$$\hat{r} = \frac{r}{r_g/2} = \frac{r}{GM/c^2}, \tag{40}$$

where r_g is the Schwarzschild radius.

(b) Frequency of Vertical Oscillations, $\Omega_\perp$

Another important frequency characterizing the disk oscillations is the frequency of the vertical oscillations of fluid particles, $\Omega_\perp$, around the equatorial plane. In Newtonian disks the frequency is equal to the Keplerian one $\Omega_K (= GM/r^2)$. This is also the case in relativistic disks with non-rotating central objects, if the relativistic Keplerian frequency is adopted. In relativistic disks with a rotating central object, however, it is no longer equal to the Keplerian one and becomes (Kato 1990)

$$\Omega_\perp^2 = \Omega_K^2\left(1 - \frac{4a}{\hat{r}^{3/2}} + \frac{3a^2}{\hat{r}^2}\right), \tag{41}$$

where Ω_K is the relativistic Keplerian frequency defined by

$$\Omega_K^2 = \frac{GM}{r^3}\left[1 + \frac{a}{(8\hat{r}^3)^{1/2}}\right]^{-1}. \tag{42}$$

The radial distributions of $\kappa(r)$ and $\Omega_\perp(r)$ are shown in figure 3, with Ω_K, for some values of the rotation parameter a (see also Perez et al. 1997).

(c) *Dispersion Relation*

A general derivation of the dispersion relation in relativistic disks is complicated. The physical arguments made in the previous section, however, suggest that the essential part of the wave phenomena can be described by replacing the Newtonian κ and Ω_K in the dispersion relation (34) by the relativistic κ and $\Omega_\perp$, respectively,

$$(\tilde{\omega}^2 - \kappa^2)(\tilde{\omega}^2 - n\Omega_\perp^2) = \tilde{\omega}^2 c_s^2 k_r^2. \tag{43}$$

Here, κ is given by equation (39), and $\Omega_\perp$ by equation (41). Equation (43) was derived based on a simple physical argument by Kato (1990). More correct forms of the dispersion relation have been derived by Ipser (1994, 1996), Perez et al. (1997), Silbergleit et al. (2000), as mentioned before.

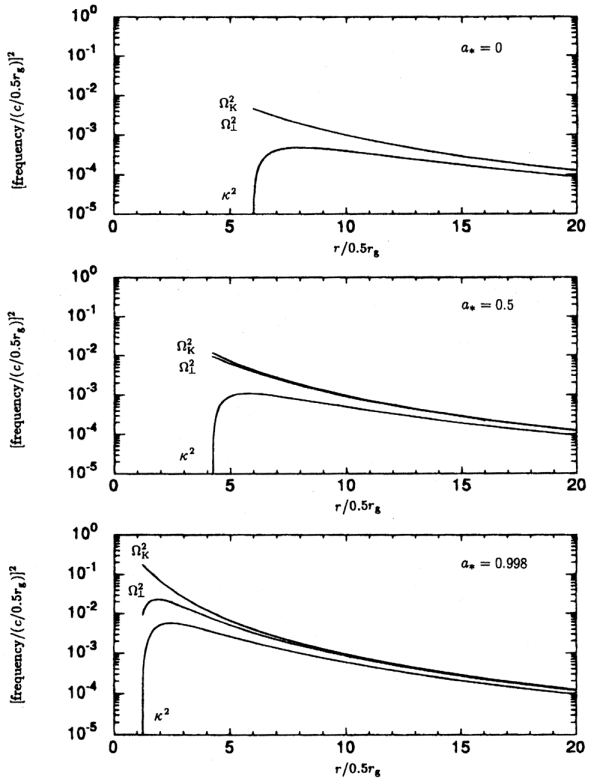

Fig. 3. The radial distributions of $\kappa(r)$, $\Omega_\perp(r)$, and $\Omega_K(r)$ for a (rotational parameter) = 0.0, 0.500, and 0.998. (After Perez et al. 1997. See also Kato et al. 1998)

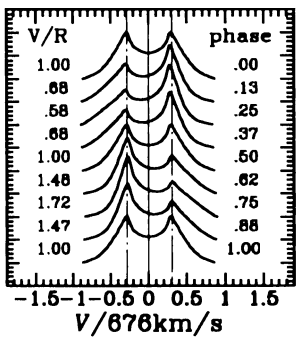

Fig. 4. Example of calculations of line-profile variations due to $m = 1$ perturbations superposed on Be star envelopes. On both sides of each profile, the V/R ratio and the phase are given. The vertical dash-dotted line denotes the peak velocities of the unperturbed profiles. See Okazaki (1996) for parameter values describing the unperturbed disks and so on. (After Okazaki 1996)

4. Low-Frequency Global Oscillations

In geometrically thin disks the strongest restoring force which makes the perturbations oscillatory is that due to rotation. The characteristic frequency of this restoring force is the epicyclic frequency κ. The radial distribution of $\kappa(r)$ is thus important in determining such wave phenomena as trapping, as discussed in the next section. When there is no trapping, however, the wavelength of perturbations generally becomes very short as they propagate outward for the following reasons. Let us consider an axisymmetric ($m = 0$) inertial–acoustic wave whose frequency is ω, and assume that the dispersion relation (34) is satisfied with a relatively small k_r at a radius. As the wave propagates outward, the values of Ω_K and κ decrease appreciably. Hence, the dispersion relation cannot generally be satisfied unless $c_s^2 k^2$ changes as the order of Ω_K. Since we are considering geometrically thin disks, $c_s^2 k^2 \sim \Omega_K^2$ means $1/k \sim H \ll r$.

Such short-wavelength oscillations are, however, uninteresting from both theoretical and observational points of view, since they do not grow to a large amplitude by phase-mixing and viscous and thermal dissipations. This consideration suggests that interesting phenomena in disks are (i) global oscillations which are realized by some particular situations or (ii) trapped oscillations. The former is discussed here, and the latter possibility is discussed in the subsequent section.

There are two kinds of wave modes which can become global. They have at the same time, low frequencies. They are (1) a one-armed ($m = 1$) inertial–acoustic wave with $n = 0$ (Kato 1983), and (2) a one-armed, inertial–acoustic wave with $n = 1$ (Kato 1989). The former is an eccentric deformation of the disk plane, and the latter is a corrugation wave.

4.1. *Eccentric Deformation of Disks*

Let us first consider the former case, i.e., $m = 1$ and $n = 0$. The dispersion relation in the lowest order of WKB approximations is then

$$(\omega - \Omega)^2 - \kappa^2 = k_r^2 c_s^2. \tag{44}$$

We first consider non-relativistic disks. Since ω is low, as shown below, $(\omega - \Omega)^2 - \kappa^2$ can be approximated as $-2\omega\Omega + \Omega^2 - \kappa^2$, neglecting ω^2. We then have

$$\omega \sim -\frac{1}{2}\Omega\left(\frac{k_r c_s}{\Omega}\right)^2 + \frac{1}{2}\Omega\frac{\Omega^2 - \kappa^2}{\Omega^2}. \tag{45}$$

4.1.1. *Keplerian disks*

First, the Keplerian disks where the difference between Ω and Ω_K in the unperturbed state is balanced by the pressure force is considered. Since

$$-\frac{1}{\rho_0}\frac{dp_0}{dr} + (\Omega^2 - \Omega_K^2)r = 0, \tag{46}$$

we find that $\Omega^2 - \kappa^2$ is of the order of $\max[c_s^2/(\ell r), c_s^2/\ell^2] \sim c_s^2/(\ell r)$, where ℓ is the characteristic radial scale by which the pressure changes appreciably. Since $k_r \ell$ is generally larger than unity, we can approximate equation (45) as (Kato 1983)

$$\omega \sim -\frac{1}{2}\Omega\left(\frac{k_r c_s}{\Omega}\right)^2. \tag{47}$$

This one-armed (or eccentric) oscillation of the nearly Keplerian disks is retrograde and the frequency is smaller than the Keplerian frequency Ω_K by a factor of $(k_r c_s/\Omega)^2$, which is $(k_r H)^2$ and much smaller than unity in geometrically thin disks.

The reason why one-armed ($m = 1$) inertial–acoustic oscillations with $n = 0$ are a low-frequency global pattern is as follows (Kato 1983; Kato et al. 1998). Let us consider a cold

non-relativistic Keplerian disk, and superpose on the disk a weak large-scale density pattern of $m = 1$. The superposition of such a pattern is possible by introducing particles having eccentric orbits. In collisionless disks with a Newtonian point source, the eccentric orbits of particles are closed after one revolution. The period of the revolution is the same as that of a circular orbit as long as the mean radius of the orbit is the same. Hence, a pattern of $m = 1$ is maintained stationary on the disk without any further deformation. Actual gaseous disks, however, have pressure. The pressure force changes the rotation from a purely Keplerian one, which distorts the one-armed global pattern. The pressure has, however, another effect. It acts so as to make independent oscillations at various radii coherent as a whole. This is realized, since the deviation from the Keplerian rotation due to the pressure force is weak. The global pattern, however, rotates in order to maintain the coherence. The rotation of the coherent pattern is very weak, since the coherence of the oscillations is the results of pressure and the pressure-restoring force is much weaker than the restoring force due to rotation in geometrically thin disks. In this way, the one-armed pattern is a global-oscillation mode whose frequency ω is extremely low compared with the Keplerian frequency $\Omega_{\rm K}$.

This type of eccentric oscillations of disks is suggested to be the cause of the V/R variations of Be stars (Kato 1983; Okazaki, Kato 1985; Okazaki 1991). In many Be stars, the so-called V/R variations (time variations of the ratio of violet and red emission components) have been observed. The periods of the variations range from years to decades. The average period is ~ 7 yr (Copeland, Heard 1963; Hirata, Hubert-Delplace 1981). Okazaki (1996) demonstrated that the variations of emission-line profiles from the Be-star envelopes can actually be explained consistently by the picture of one-armed deformation of the disks. Figure 4 is an example of line-profile variations calculated by Okazaki [see Okazaki (1996) for details].

Excitation of these one-armed (eccentric) oscillations in the Be-star envelopes by viscous processes has been discussed by Okazaki (2000) and Negueruela et al. (2000). See section 7 for a general argument on the excitation of disk oscillations by viscous processes.

4.1.2. Tidally deformed disks

The above arguments show that the presence of eccentric global oscillations is quite generally expected when the disks are weakly deviated from the Keplerian ones. Actually, there is another example of derivation from the Keplerian disks. In binary systems the accretion disk surrounding the primary star is in a gravitational field whose time average is slightly deviated from $-GM/r$ by the presence of a secondary star of mass M_2. Here, M is the mass of the primary and r is the equatorial distance of a point on the disk from the primary. The time-averaged gravitational potential $\psi(r)$ on the equatorial plane of the disk is then given by

$$\psi(r) \simeq -\frac{GM}{r} - \frac{1}{4}\frac{GM_2}{d}\left(\frac{r}{d}\right)^2, \tag{48}$$

where d is the separation between the primary and secondary stars. Since

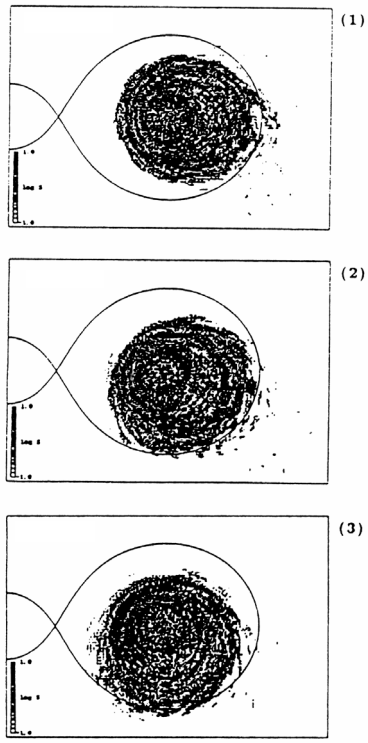

Fig. 5. Density contours on a disk surrounding the primary star in a binary system, obtained by SPH simulations. This figure has been drawn in a frame corotating with the orbital revolution. The solid curve represents the critical Roche lobe. The three panels show a sequence of the disk evolution during a 1/4 phase of the superhump period. The eccentric disk rotates in the opposite direction to the orbital revolution. If it is observed from the inertial frame, however, it slowly rotates in the same direction as the orbital motion (of the binary) and the disk rotation. (After Hirose, Osaki 1990)

$$\Omega^2 \sim -\frac{d\psi}{rdr} \simeq \frac{GM}{r^3} - \frac{1}{2}\frac{GM_2}{d^3}, \tag{49}$$

we have

$$\frac{\Omega^2 - \kappa^2}{\Omega^2} \sim \frac{3}{2}\left(\frac{r}{d}\right)^3\left(\frac{M_2}{M}\right). \tag{50}$$

That is, equation (45) gives (see also Osaki 1985)

$$\omega \sim -\frac{1}{2}\Omega\left(\frac{k_r c_{\rm s}}{\Omega}\right)^2 + \frac{3}{4}\Omega\left(\frac{r}{d}\right)^3\left(\frac{M_2}{M}\right). \tag{51}$$

Here, the first term on the right-hand side is generally negligible compared with the second term, and thus this one-armed (eccentric) pattern is prograde. This eccentric deformation of disks with slow prograde rotation was first pointed out by Osaki (1985) to be the cause of superhump phenomena in dwraf novae. Determinations of eigenfunction and eigenfrequency by detailed global mode analyses were made by Hirose and Osaki (1993) for the case of the disks of SU UMa-type dwarf novae. An example of SPH simulations, demonstrating a slow prograde rotation of a one-armed deformation of disks, is given in figure 5.

It is known by numerical simulations (Whitehurst 1988; see also Hirose and Osaki 1990) that the above eccentric deformation mode of disks can be excited by a tidal instability. The

detailed mechanism of this tidal instability has been clarified by Lubow (1991) to be the eccentric Lindblad resonance. Hirose and Osaki (1990) had shown that this instability is a parametric resonance instability in the limit of collisionless disks.

4.2. *Low-Frequency Corrugation Waves*

In relativistic disks the epicyclic frequency κ is no longer close to $\Omega_{\rm K}$, even in Keplerian disks. The eccentric deformation of disks ($m = 1$, $n = 0$) is thus not a low-frequency global pattern on the disks, unlike the Newtonian disks. In spite of this, there are still low-frequency oscillation modes on disks, if the rotation of the central source is slow; i.e., $a \ll 1$. These are one-armed ($m = 1$) corrugation waves ($n = 1$).

In the case of $m = n = 1$, the dispersion relation (34) is written explicitly as

$$\left[(\omega-\Omega)^2-\kappa^2\right]\left[(\omega-\Omega)^2-\Omega_\perp^2\right]=(\omega-\Omega)^2c_{\rm s}^2k_r^2. \qquad (52)$$

First, we briefly discuss the Newtonian Keplerian disks, although our main interest in this subsection is relativistic disks. In Newtonian disks, $\Omega \sim \Omega_{\rm K} \sim \kappa$ and $\Omega_\perp = \Omega_{\rm K}$. Hence, we have

$$(\omega-\Omega)^2-\kappa^2 \sim -2\omega\Omega \ \text{ and } \ (\omega-\Omega)^2-\Omega_\perp^2 \sim -2\omega\Omega, \qquad (53)$$

when ω is sufficiently low. If these approximations are adopted (the following results actually show that these approximations hold when $k_r H \ll 1$), equation (52) gives

$$\omega \sim \pm\frac{1}{2}k_r c_{\rm s}. \qquad (54)$$

This shows that the waves tilting (warping) the disk plane propagate in the radial direction roughly with acoustic speed, although the disk is rotating rapidly.

We next consider relativistic disks. In this case the first approximation of equations (53) no longer holds, since $\kappa^2 \ll \Omega^2$. The closeness of the frequency of the vertical oscillation, $\Omega_\perp$, and the frequency of disk rotation, Ω, however, still holds if the rotation of the central object is slow, i.e., $a \ll 1$. This closeness gives us low-frequency oscillations. That is, by assuming $(\omega-\Omega)^2-\Omega_\perp^2$ as $-2\omega\Omega+(\Omega^2-\Omega_\perp^2)$ and $(\omega-\Omega)^2-\kappa^2$ as $\Omega^2-\kappa^2$, we have from the dispersion relation (52)

$$\omega \sim -\frac{1}{2}\Omega\frac{\Omega^2}{\Omega^2-\kappa^2}\frac{k_r^2c_{\rm s}^2}{\Omega^2}+\frac{1}{2}\Omega\frac{\Omega^2-\Omega_\perp^2}{\Omega^2}. \qquad (55)$$

Since $k_r^2c_{\rm s}^2/\Omega^2 \ll 1$ and $(\Omega^2-\Omega_\perp^2)/\Omega^2 \ll 1$, this dispersion relation (55) shows that even in the innermost region of rapidly rotating relativistic disks, there are very low-frequency modes of oscillations, whose frequencies are much smaller than Ω.

The difference between Ω^2 and $\Omega_{\rm K}^2$ is of the order of $c_{\rm s}^2/(\ell r)$, where ℓ is the characteristic radial scale by which the pressure changes appreciably. Hence, if $(k_r r)(k\ell) > 1$, we can neglect the second term on the right-hand side of equation (55) when $a \ll 1$. The pattern of the oscillations then slowly rotates in the direction opposite to the disk rotation. The frequency is smaller than Ω by the order of $(k_r H)^2 (\ll 1)$, which is even smaller than the frequency given in equation (54) by $k_r H$.

The reason why the one-armed corrugation waves have a low frequency when $a \ll 1$ can be understood as follows (Kato 1989). Let us consider the displacement of a particle from the equatorial plane in the vertical direction. The particle feels a gravitational restoring force toward the equator, which is $\Omega_\perp^2 \xi_z$ when the vertical displacement ξ_z is small. Hence, the particle undertakes harmonic oscillations around the equatorial plane with frequency $\Omega_\perp(r)$. This frequency is close to the Keplerian frequency $\Omega_{\rm K}(r)$ when the spin of the central source is slow. In other words, the vertical oscillation period of the particle coincides with the period by which the particle rotates around the central object. This means that in the limit of no temperature and $a = 0$ a one-armed corrugation pattern is maintained with little time change. If $\Omega_\perp = \Omega_{\rm K}$ does not hold, however, the deformed pattern is no longer maintained steadily. The pattern changes with time at each radius independently. Against this incoherent time change, the pressure force acts so as to keep the pattern global and coherent. We can thus expect a low-frequency global corrugation pattern on disks. This effect of pressure is similar to that in the case of an eccentric deformation of Newtonian disks (see subsection 4.1).

Here, we should note the differences of the corrugation waves from other types of warps (or tilts). In a collisionless non-selfgravitating disk, the precession of the disk plane is independent at each radius. That is, the frequency of precession is a function of the position, and thus the precession, itself, is not a coherent motion. For the precession to become a coherent global motion, pressure, viscosity, or self-gravity is necessary. The coherent motions under the action of self-gravity have been studied in galactic warps (e.g., Nelson, Tremaine 1995) and those due to viscosity have been examined extensively in the field of accretion disks (e.g., Papaloizou, Pringle 1983; Pringle 1996; Markovic, Lamb 1999; Ogilvie 1999). Coherent warp motions considered here are due to pressure, different from those due to self-gravity and viscosity.

Observational evidence suggesting warps (or tilts) of disk planes have been accumulating in recent years in AGNs (Miyoshi et al. 1995) and X-ray binaries (Maloney, Begelman 1997). Some of them might be the warps considered here (i.e., corrugation waves).

When the spin parameter a is not small, the difference between $\Omega_{\rm K}^2$ and $\Omega_\perp^2$ is not small, and thus one-armed corrugation waves are no longer low-frequency, global deformations of disks. The one-armed corrugation waves in general relativistic disks have been studied extensively by Silbergleit et al. (2000) under the Kerr metric.

5. Trapped Oscillations in Relativistic Disks

The disks have no definite outer boundary in the radial direction. Oscillations and waves are thus propagated away in the radial direction and will not grow to observable amplitudes, unless there are reflection boundaries. In this sense, trapping of oscillations in a limited region is an interesting issue to be studied. This is the subject in this section.

5.1. *Fundamental Mode ($n = 0$)*

Let us consider here, for simplicity, axially symmetric oscillations, i.e., $m = 0$ and thus $\tilde{\omega}^2 = \omega^2$. Furthermore, we first consider the fundamental mode ($n = 0$) in the vertical direction. The dispersion relation then gives $\omega^2 = \kappa^2 + c_{\rm s}^2 k_r^2$, and the region where the waves can propagate is specified by

$$\omega^2 > \kappa^2, \qquad (56)$$

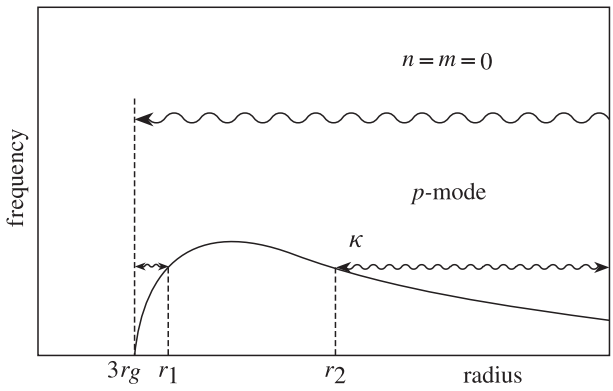

Fig. 6. Schematic diagram showing the radial region where waves of axisymmetric fundamental mode ($m = 0$, $n = 0$) can propagate on relativistic disks. For waves with $\omega < \kappa_{\max}$, the propagation region is separated into two portions: $3r_g < r < r_1$ and $r > r_2$. In Newtonian disks there is no inner propagation region of waves (see figure 1). (After Kato et al. 1998)

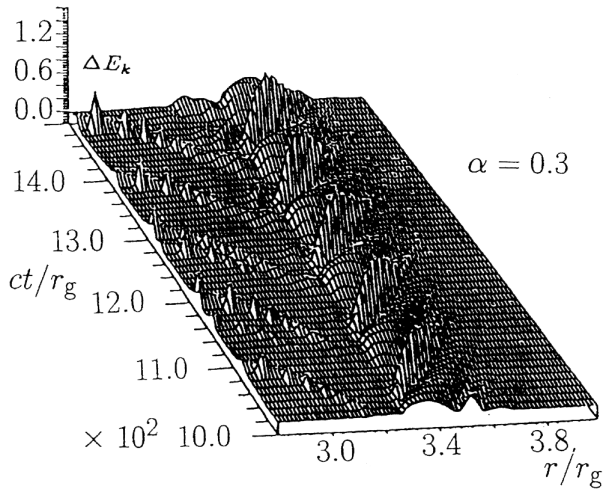

Fig. 7. Time variation of the kinetic energy E_K ($\equiv \Sigma u_r^2/2$) of the radial motion in the case of isothermal disks with c_T(isothermal sound speed) $= 10^{-3}c$, $\alpha = 0.3$, and $\dot{M}/\dot{M}_{crit} = 1.6$, where $M_{crit} = L_E/c^2$ using the Eddington luminosity L_E. Here Σ is the surface density and E_K is normalized in units of $\Sigma_c c_T^2$, Σ_c being the surface density at the critical radius $r_c \sim 3r_g$. It is shown that the outward propagation of perturbations is blocked around the radius $3.8r_g$ by the barrier of the epicyclic frequency. That is, the oscillations are restricted in the innermost region of the disk. It is also shown that the gas falls into the central object quasi-periodically. (After Matsumoto et al. 1988. See also Kato et al. 1998)

since k_r^2 must be positive. Figure 6 shows schematically the region where this condition is satisfied. An important result is that the wave propagation region is separated into two regions (inner region of $r < r_1$ and outer region of $r > r_2$) when $\omega < \kappa_{\max}$, although the wave-propagation region is the entire region of the disks when $\omega > \kappa_{\max}$. This separation of the propagation region when $\omega < \kappa_{\max}$ is due to general-relativistic effects.

Wave propagating inward from a far outer region with a frequency ω ($< \kappa_{\max}$) is considered. As the wave approaches radius r_2, where $\kappa = \omega$ is realized, the wavelength of the wave increases and finally becomes infinite ($k_r = 0$) at $r = r_2$ as far as the local dispersion relation is concerned (see that the dispersion relation is given by $\omega^2 = \kappa^2 + c_s^2 k_r^2$). This means that the waves are reflected back outward at $r = r_2$. If $\omega^2 > \kappa_{\max}^2$, on the other hand, the waves can propagate inward until the inner edge of the disk. This is in contrast with the case of non-relativistic disks, in which the epicyclic frequency increases monotonically inward without any limit so that all waves should be reflected back outward at a radius where $\omega^2 = \kappa^2$ is realized if r_b is sufficiently small (see figure 1).

More importantly, there is a wave-propagation region in the innermost region of disks when $\omega < \kappa_{\max}$, and waves can be trapped there (Kato, Fukue 1980). Let us consider an inertial–acoustic wave propagating outward in the region just outside the inner edge ($\sim$ the radius of the marginally stable circular orbit, r_{ms}, and close to $3r_g$ when $a \sim 0$). If $\omega < \kappa_{\max}$, the wave is reflected back inward by the wall of the epicyclic frequency at $r = r_1$. A wave propagating inwards toward the inner edge, on the other hand, would be partially reflected back outward at the inner edge, since the inner edge of disks is a sharp boundary where the density decreases sharply inward. Because of this, the waves transported there with accretion flow are partially reflected back as outgoing acoustic waves by the following situations. Just outside the sonic radius, the inward-propagating inertial–acoustic wave is linearly coupled with the other perturbation modes (the outward-propagating inertial–acoustic mode, thermal and viscous modes) due to strong inhomogeneity of the disk structure (Kato et al. 1988a, b). That is, an outward-propagating inertial–acoustic mode is generated there. This generated wave is roughly standing at first, since the inner edge is near the sonic radius. This standing wave begins to propagate outward after growing to a certain level. This phenomenon can be regarded as the reflection of the inward-propagating wave into an outward-propagating wave.

It is noted here that the reflection of perturbations at the inner edge does not occur only to the inward-propagating acoustic waves. A thermal mode transported inward by accretion flow is also reflected back at the inner edge as an outward-propagating acoustic wave. The reason for the reflection is similar to the case of inward-propagating acoustic waves in the sense that the thermal mode is linearly coupled with the other modes around the inner edge by the strong inhomogeneity of the disk structure. This reflection of the thermal mode into an outgoing-acoustic wave has been demonstrated by Manmoto et al. (1996) by numerical simulations.

Before closing this subsection, we summarize the simulation results of disk oscillations made so far. Time-dependent numerical simulations to examine how axisymmetric fundamental ($n = 0$) p-mode perturbations are trapped in the inner region of viscous disks were first made by Matsumoto et al. (1988, 1989) with quasi-Newtonian potential and the standard α-viscosity. These studies are extended by Honma et al. (1992) and Chen and Taam (1995). Milsom and Taam (1997) further extended them to cases of two-dimensional disks. As examples of these simulation results, those by Matsumoto et al. (1988) are shown in figures 7 and 8.

Interesting results obtained by these simulations are that (1) wavy perturbations are generated and trapped in the innermost region of the disks (between the inner edge and a certain

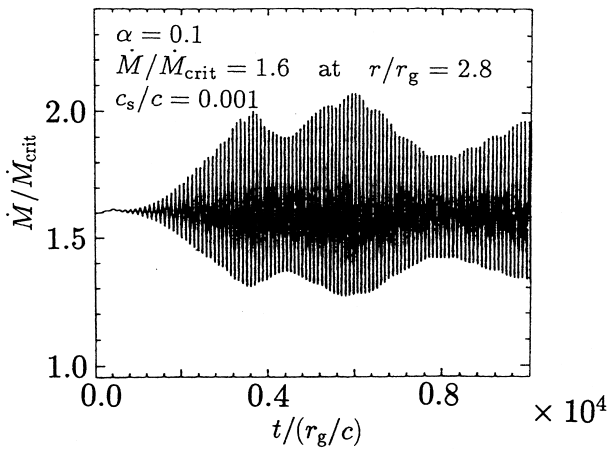

Fig. 8. Time variation of the accretion rate at $r/r_{\rm g} = 2.8$ (inside the sonic radius) in the case of isothermal disks with $c_{\rm T}/c = 10^{-3}$. The values of $\alpha = 0.1$ and $\dot{M}/\dot{M}_{\rm crit} = 1.6$ have been adopted. Quasi-periodic oscillations are observed, whose period is roughly $10^{-3}(M/M_\odot)$ s, which corresponds to $\kappa_{\rm max}$ in frequency. In the case of isothermal disks, the amplitude of oscillations modulates with the timescale by which acoustic waves travel across the trapped region of oscillations. (After Matsumoto et al. 1988. See also Kato et al. 1998)

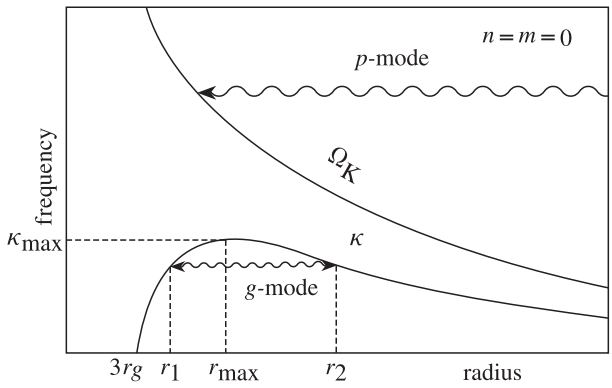

Fig. 9. Schematic picture showing the trapping of axisymmetric inertial–gravity modes with $n = 1$ in the region between r_1 and r_2. Below the curve of $\kappa(r)$ g-mode waves can exist, while p-mode waves can exist only in the right-upper region of the curve $\Omega_{\rm K}(r)$. (After Kato et al. 1998)

radius of a few $r_{\rm g}$). The outer edge of the trapped region changes insignificantly as the disk evolves, but depend somewhat on parameters adopted. For example, the outer edge is about $6r_{\rm g}$ in a case of Chen and Taam (1995), while it is about 3.5–4.0 $r_{\rm g}$ in cases by Honma et al. (1992). The second important results is that (2) the spectrum analyses of the trapped oscillations show quasi-periodic oscillations whose frequency is close to $\kappa_{\rm max}$. This is a rather general fearuture of oscillations in the innermost region of geometrically thin relativistic disks (see chapter 15 of Kato et al. 1998 for a review).

Linear eigenmode analyses of trapped oscillations in low-temperature disks suggest that the trapped region is much narrower near to the inner edge and the frequency of the trapped oscillations is lower than $\kappa_{\rm max}$ (Kato, Fukue 1980). The results of numerical simulations are, however, distinct from those of linear eigenmode analyses. The physical reasons for the difference are not clear. One of the reasons could be that the phase mixing of waves is little in those waves having a long wavelength. Furthermore, vanishing of the group velocity for waves of $\omega = \kappa_{\rm max}$ or some non-linear behavior of excited oscillations might be related to the dominance of quasi-periodic oscillations of $\sim \kappa_{\rm max}$. Further considerations are necessary.

As mentioned below, the first overtone ($n = 1$) of g-modes also becomes trapped oscillations with frequencies of $\sim \kappa_{\rm max}$.

5.2. *First Overtone ($n = 1$)*

Let us next consider the axially-symmetric ($m = 0$) first overtone ($n = 1$) in the vertical direction. As shown in equation (43) and described before, there are two wave modes. One is the inertial–gravity waves (g-mode), the square of whose frequency, ω^2, is smaller than κ^2, i.e.,

$$\omega^2 < \kappa^2. \tag{57}$$

The other is inertial–acoustic waves (p-mode), the square of whose frequency, ω^2, is larger than $\Omega_{\rm K}^2$:

$$\omega^2 > \Omega_{\rm K}^2. \tag{58}$$

We consider the former mode of inertial–gravity waves. Since κ has a maximum at a certain radius, say $r_{\rm max}$, and decreases both inward and outward, the propagation region of the waves with frequencies $\omega < \kappa_{\rm max}$ is restricted to within a finite region ($r_1 < r < r_2$) around $r_{\rm max}$, as shown in figure 9. This means that we can expect trapped oscillations of inertial–gravity waves in the region around $r_{\rm max}$ with frequencies of $\sim \kappa_{\rm max}$ (Okazaki et al. 1987; Nowak, Wagoner 1992; Perez et al. 1997).

A characteristic nature of this trapped oscillations is that their frequencies are insensitive to changes of the disk structure as long as the disks are moderately geometrically thin. This is because $\kappa_{\rm max}$ depends only on the mass of the central black hole in the Keplerian disks. As an inspection of equation (39) shows, $\kappa_{\rm max} \propto 1/M$ since $r_{\rm g} \propto M$. Detailed calculations of the eigenfrequency ω of the trapped g-mode oscillations have been made by Perez et al. (1997), using the Kerr geometry. The spatial behavior of the eigenfunction of these trapped oscillations is shown, for example, by figure 5 by Nowak and Lehr (1998).

The resultant oscillation frequency f is (Nowak et al. 1997)

$$f = 700 \left(\frac{M}{M_\odot}\right)^{-1} F(a)(1-\epsilon) \ \text{Hz}, \tag{59}$$

where ϵ is a small correction factor involving a disk thickness, and radial and vertical mode numbers. The effects of the rotation of the central black hole appear in the factor $F(a)$, where a is a dimensionless spin parameter and $F(a)$ monotonically increases along with an increase of a from $F(0) = 1$ to $F(0.998) = 3.443$. Nowak et al. (1997) suggested that these trapped oscillations might be the origin of the 67 Hz oscillations observed in the black-hole candidate GRS 1915+105. The derived black-hole mass is $10.5M_\odot$ and $36.6M_\odot$ for the cases of a non-rotating ($a = 0$) and a maximally rotating black hole ($a = 0.998$), respectively. In figure 10 the 67 Hz oscillations found by Morgan et al. (1997) are depicted.

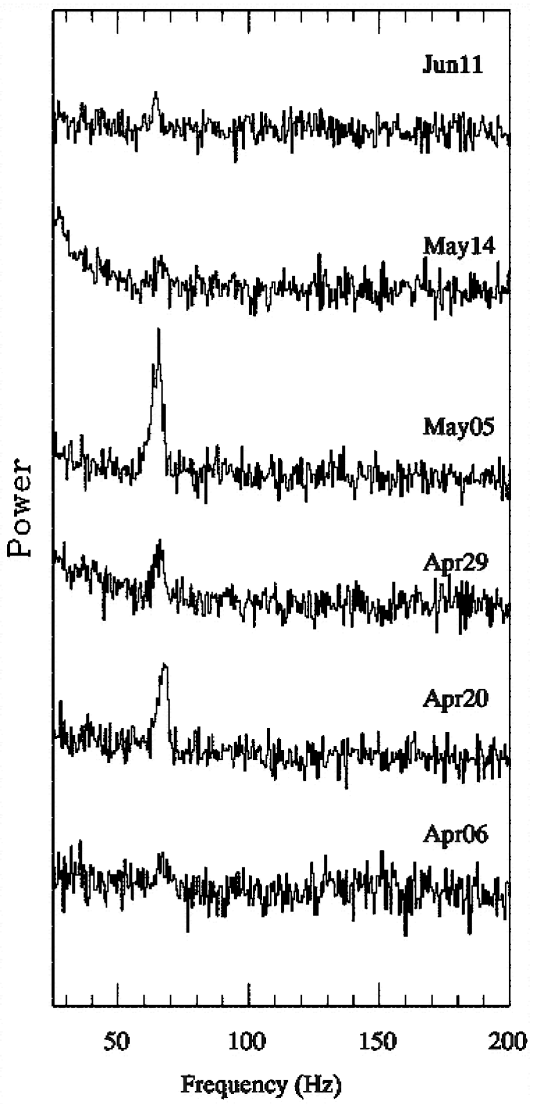

Fig. 10. Selected power spectra of GRS 1915+105 plotted on a linear scale to display the QPO at 67 Hz. Here, the Poisson noise level has not been subtracted. (After Morgan et al. 1997)

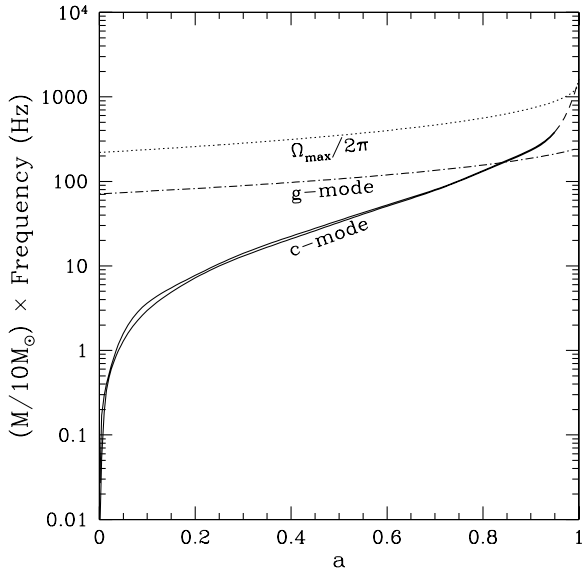

Fig. 11. Dependence of frequencies of g-mode and c-mode oscillations on the angular momentum of the black hole. The c-mode curves bound the region corresponding to the parameter ranges $0.001 \leq L/L_{\rm Edd} \leq 0.1$ and $10 \leq M/M_\odot \leq 10^9$, with $\alpha = 0.1$. (After Silbergleit et al. 2000)

5.3. *One-Armed Corrugation Waves ($m = 1$ and $n = 1$)*

Other modes of oscillations which are interesting from the viewpoint of trapping are one-armed ($m = 1$) corrugation waves ($n = 1$). Since $\Omega_\perp^2 > \kappa^2$ in relativistic disks, the propagation region of the low-frequency one-armed corrugation waves is specified by $(\omega - \Omega)^2 - \Omega_\perp^2 > 0$, i.e., by

$$\omega < \Omega - \Omega_\perp, \tag{60}$$

if the dispersion relation (52) is adopted. The trapping nature of the c-mode oscillations was examined first by using the propagation region specified by inequality (60) (Kato 1990), but it was not appropriate for the following reasons. In the case when $a \ll 1$, Ω and $\Omega_\perp$ are close to each other (see figure 3). This suggests that an examination of the propagation region of the corrugation waves by using inequality (60) must be careful, since small correction terms which were neglected in deriving the dispersion relation (52) are not always negligible compared with the difference, $\Omega - \Omega_\perp$. In other words, equation (30) describing the radial structure of perturbations and equation (31) describing the vertical structure of perturbations must be coupled and solved simultaneously, without decoupling them, like we did in deriving the dispersion relation (52).

Silbertgleit et al. (2000) made such careful examinations, and found that the one-armed corrugation waves are actually trapped in the inner region of the disks. The trapped region is wide and the eigenfrequency is low when a is small, but the region becomes narrow and the frequency is high when a is large. That is, the radial extent of the trapped region is a decreasing function of a, while the eigenfrequency of the trapped oscillations increases monotonically as the spin parameter a increases toward unity (Silbergleit et al. 2000). The a-dependence of trapped c-mode oscillations (and that of g-mode ones) derived by Silbergleit et al. (2000) are shown in figure 11. The eigenfrequency of the trapped oscillations coincides with the Lense–Thirring frequency at its outer trapping zone boundary (Silbergleit et al. 2000). This can be understood from the following situations. The Lense–Thirring frequency is the frequency of the vertical precession of a particle rotating around a rotating central object. The Lense–Thirring frequency $\Omega_{\rm LT}$ at radius r is thus the difference between $\Omega_{\rm K}$ and $\Omega_\perp$, i.e., $\Omega_{\rm LT}(r) = \Omega_{\rm K}(r) - \Omega_\perp(r)$. Equation (60), on the other hand, suggests that the outer boundary of the trapped region of the c-mode oscillations is the radius where $\omega = \Omega - \Omega_\perp$ is realized. Since $\Omega \sim \Omega_{\rm K}$ we have $\omega \sim \Omega_{\rm LT}$ at the outer boundary.

The characteristics of the various wave modes considered in sections 4 and 5 are briefly summarized in tables 1 and 2 (see section 9).

6. Viscous Excitation of Disk Oscillations

We have so far discussed the basic properties of the oscillation modes on disks. The next problem is whether such oscillations are actually excited on the disks. This issue is discussed in this and subsequent sections (sections 6 and 7).

It is well known that in non-equilibrium open systems dissipative processes can often lead the systems to unstable oscillatory states. The excitation of stellar oscillations by non-adiabatic processes are one of these typical examples. Three typical excitation mechanisms are known in stellar oscillations: κ-, ϵ-, and δ-mechanisms (Unno et al. 1989). The κ-mechanism is a process of changing the energy flowing outward as radiation into the kinetic energy of oscillations through the effects of opacity. Whether opacity variations associated with oscillations can amplify the oscillations depends on the density and temperature dependences of the opacity κ. In the ϵ-mechanism the thermal energy generated by the nuclear reaction is changed into the kinetic energy of the oscillations. A strong temperature dependence of the nuclear energy generation rate ϵ is crucial for this mechanism to act. The δ-mechanism is one of double-diffusive instabilities known in plasma physics, and is sometimes called the Cowling mechanism, since Cowling (1958) found this mechanism as a process that makes convections overstable.

The above excitation mechanisms of oscillations, of course, can operate in accretion disks, if situations favorable for the mechanisms are realized. In disk oscillations, however, other mechanisms which have not been considered in stellar pulsation become important. They are processes related to viscosity. As is well known, viscosity has two important effects on disk configurations. One is on the thermal-energy balance through viscous heat generation, and the other is on the angular-momentum balance through viscous angular momentum transport. Related to them, two additional excitation processes are of importance in disk oscillations (Kato 1978). One is a thermal process of viscosity (denoted here by process [1]) and the other is a dynamical one of viscosity (process [2]).

The former process [1] is a kind of generalization of the ϵ-mechanism. In the compressed phase of oscillations, the density, temperature, and pressure increase. This usually brings about an increase in the viscosity, and thus an increase in the viscous heat generation, leading to an increase in the pressure-restoring force. In other words, the increase of the pressure-restoring force during the compressed phase is more than that due solely to adiabatic compression. Thus, the oscillations are pushed back towards the next expansion phase with a force stronger than the adiabatic oscillations have, and the amplitude of the oscillations at the expansion phase becomes larger than that of the previous expansion phase. In the expansion phase, a similar situation occurs with the opposite sign. The amplitude of oscillations thus increases steadily with time *(overstability)*.

The latter process [2] is as follows. Let us consider, for simplicity, axisymmetric oscillations. In oscillations of rotating systems, a fluid element inevitably undergoes a time-periodic azimuthal motion during the oscillations, since the angular momentum of a given fluid element is conserved during the oscillations (in the limit of no dissipation). On the other hand, the viscous force acting on the fluid element in the azimuthal direction, say N_φ, also changes time-periodically during the oscillations. If the azimuthal component of the Lagrangian change of velocity, δv_φ, due to the oscillations and the Lagrangian change of N_φ associated with the oscillations, say δN_φ, are in phase, positive work is done on the oscillations. The oscillations then grow (see section 7). This phase matching actually occurs under a certain condition, if the viscosity increases during the compression phase of oscillations. Whether this has a sufficient magnitude to amplify the oscillations against other normal viscous damping processes depends on the characteristics of the oscillations and the density and temperature dependences of viscosity. (More detailed discussions are given later.) It is noted that a general stability analysis of a viscous rotating Newtonian fluid was recently made by Ortega-Rodriguez and Wagoner (2000), the disk instability being discussed as a special case.

In the following subsection we demonstrate the above-mentioned dynamical process of amplification (process [2]) in an idealized situation, where process [1] as well as κ-, ϵ-, and δ- processes are all filtered out, and only process [2] and the usual viscous damping processes remain.

One more important point to be emphasized here is that process [2] is strengthened when the disk is relativistic, which is also demonstrated below.

Finally, it is instructive to emphasize an analogy of process [2] to the κ-mechanism. In the κ-mechanism, as mentioned before, a part of the radiative energy flowing in the radial direction (in the case of stars) is transferred to kinetic energy of oscillations through the effects of opacity κ. In process [2], on the other hand, a part of the energy associated with the angular momentum flowing in the radial direction is transferred to kinetic energy of oscillations through the effects of viscosity η. In this sense, it is suitable to call process [2] the η-mechanism. The fact that process [2] is strengthened in relativistic disks is also understandable from this point of view, since the angular-momentum transport by viscosity is related to the radial gradient of the angular velocity of rotation, Ω (which is larger in magnitude in relativistic disks), while the frequency of oscillations is related to the epicyclic frequency (which is smaller in relativistic disks).

6.1. *Local Inertial–Acoustic Oscillations in Isothermal Disks*

The main part of this subsection is a duplicate of Kato et al. (1998). To demonstrate the dynamical effects of viscosity (process [2]) on excitation of disk oscillations, we consider axially-symmetric ($\partial/\partial\varphi = 0$) isothermal perturbations on isothermal disks. The perturbations considered here are inertial–acoustic oscillations with no node ($n = 0$) in the vertical direction, since the viscous excitation of disk oscillations is clearly demonstrated in this case. In order to demonstrate the essential part of process [2], the oscillations are further taken to be local in the sense that their radial wavelength λ is much shorter than the radial scale of the disk. The radial wavelength λ is, however, assumed to be longer than the disk thickness, i.e., $H \ll \lambda \ll r$. Since the oscillations are nearly horizontal, we neglect both the vertical component of the perturbed motions and the vertical derivation of the perturbed quantities, i.e., $u_z = 0$ and $\partial/\partial z = 0$.

The equation of continuity describing the local oscillations

is then

$$\frac{\partial}{\partial t}\left(\frac{\rho_1}{\rho_0}\right)+\frac{\partial u_r}{\partial r}=0. \tag{61}$$

Quantities attached by the subscripts 0 and 1 denote, respectively, those of the unperturbed disk and those perturbed by oscillations. Since we consider isothermal perturbations on the isothermal disk, the energy equation is replaced by

$$p_1=c_{\rm T}^2\rho_1, \tag{62}$$

where $c_{\rm T}$ is the isothermal sound speed.

The r- and φ-components of the equation of motion are written, respectively, as

$$\frac{\partial u_r}{\partial t}-2\Omega u_\varphi=-c_{\rm T}^2\frac{\partial}{\partial r}\left(\frac{\rho_1}{\rho_0}\right)+\frac{1}{\rho_0}\frac{\partial t_{rr,1}}{\partial r}, \tag{63}$$

$$\frac{\partial u_\varphi}{\partial t}+\frac{\kappa^2}{2\Omega}u_r=\frac{1}{\rho_0}\frac{\partial t_{r\varphi,1}}{\partial r}, \tag{64}$$

where $t_{rr,1}$ and $t_{r\varphi,1}$ are, respectively, the perturbed parts of the rr- and $r\varphi$-components of the viscous stress tensor. The $r\varphi$-component $t_{r\varphi}$ is written in the form

$$t_{r\varphi}=\eta r\frac{\partial}{\partial r}\left(\frac{v_\varphi}{r}\right), \tag{65}$$

where η is the dynamical viscosity due to turbulence and v_φ is the azimuthal component of velocity; $v_\varphi=r\Omega+u_\varphi$. Since local perturbations are considered, we have

$$\frac{\partial t_{r\varphi,1}}{\partial r}=\frac{\partial \eta_1}{\partial r}r\frac{d\Omega}{dr}+\eta_0\frac{\partial^2 u_\varphi}{\partial r^2}. \tag{66}$$

Similarly, we have

$$\frac{\partial t_{rr,1}}{\partial r}=\frac{4}{3}\eta_0\frac{\partial^2 u_r}{\partial r^2}. \tag{67}$$

The viscosity η is taken here to be

$$\eta=\frac{\alpha\rho c_{\rm T}^2}{\Omega}, \tag{68}$$

which is the conventional description of turbulent viscosity and α is a dimensionless constant ($\alpha<1$). The perturbed part of this equation gives

$$\frac{\eta_1}{\eta_0}=A\frac{\rho_1}{\rho_0}, \tag{69}$$

with $A=1$, since isothermal perturbations are considered here. Although $A=1$, A is retained here unspecified in order to see how a viscosity variation influences the final result of the growth rate.

Equations (61)–(64), (66), (67), and (69) are the set of equations describing local linear perturbations. We solve these equations under the condition that all perturbed quantities are proportional to $\exp[i(\omega t-kr)]$, where k is a given radial wavenumber. In this examination, the effects of viscosity on oscillations are taken into account as perturbations. That is, we adopt a quasi-inviscid approximation and all perturbed quantities associated with the oscillations are expanded by a power series with respect to the effects of viscosity; e.g.,

$$u_r=u_r^{(0)}+u_r^{(1)}+\ldots, \quad \text{and} \quad \omega=\omega^{(0)}+\omega^{(1)}+\ldots \tag{70}$$

Then, the zeroth-order equations describing the oscillations with no viscosity give the wave equation,

$$\left(\frac{\partial^2}{\partial t^2}-c_{\rm T}^2\frac{\partial^2}{\partial r^2}+\kappa^2\right)u_r^{(0)}=0. \tag{71}$$

This equation gives the zeroth-order dispersion relation,

$$\left[\omega^{(0)}\right]^2=\kappa^2+c_{\rm T}^2k^2. \tag{72}$$

The differential equations describing the next-order quantities are solved by applying a compatibility condition, as is usually done in the perturbation method. This condition gives $\omega^{(1)}$. The results show that $\omega^{(1)}$ is purely imaginary, and thus the oscillations grow or damp by the effects of viscosity. From the detailed expression for $\omega^{(1)}$, the growth rate G is found to be (e.g., Kato et al. 1998)

$$G=-\Im(\omega^{(1)})=-\frac{\eta_0}{\rho_0}k^2\left[\frac{\Omega^2}{\kappa^2+c_{\rm T}^2k^2}\left(A\frac{d\ln\Omega}{d\ln r}+\frac{\kappa^2}{2\Omega^2}\right)+\frac{2}{3}\right], \tag{73}$$

where $\Im$ denotes the imaginary part.

Among three terms in the brackets on the right-hand side of equation (73), the first two come from $t_{r\varphi,1}$ and the third one from $t_{rr,1}$. This shows that the effects of the rr-component of the stress tensor are always to dampen the oscillations, but that the effects of the $r\varphi$-component are not always to do so. That is, the effects of a time change of the viscosity (represented by the first term proportional to A) acts so as to amplify the oscillations against the effects of the other damping processes of the viscosity, since $d\ln\Omega/dr<0$. The non-relativistic Keplerian disks are in a marginal state (slightly unstable), since $\Omega^2/(\kappa^2+c_{\rm s}^2k^2)\sim\Omega^2/\kappa^2\sim1$ and $d\ln\Omega/d\ln r=-3/2$. Relativistic disks are, however, strongly unstable, since $\Omega^2/\kappa^2>1$ and $d\ln\Omega/d\ln r<-3/2$. Both the smallness of κ^2 compared with Ω^2 and the largeness of $|d\ln\Omega/d\ln r|$ contribute to the instability in relativistic disks.

The growth rate given by equation (73) is shown in figure 12 as functions of r, when the rotation is the Keplerian one ($\Omega=\Omega_{\rm K}$) under a pseudo-Newtonian potential (Paczyński, Wiita 1980) and $c_{\rm T}^2k^2=0.1\Omega_{\rm K}^2$. For a comparison, the growth rate G in the case of the Newtonian potential is also shown with the same parameters. It should be noticed that the relativistic disks are strongly unstable in the innermost region.

Distinct from the above excitation of $n=0$ oscillations, process [2] does not always act in the direction of excitation of the oscillations when $n\neq0$. Before showing this, we derive a general instability criterion in the next section.

7. A General Criterion of Oscillatory Instability

Viscous excitation of disk oscillations was first shown by Kato (1978) and Blumenthal et al. (1984) by using Eulerian variables. To derive perspectively a general form of the stability criterion, however, the adoption of Lagrangian variables is better. In this section we derive a general criterion of an oscillatory instability (overstability) of geometrically thin disks by using the Lagrangian variables. The basic assumptions involved in this formulation are that the unperturbed disks are steady isolated systems. The isolation implies that the

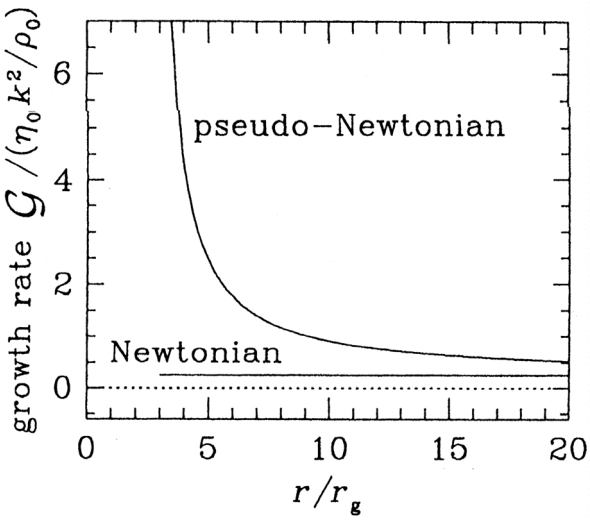

Fig. 12. Growth rate G of axially-symmetric ($m = 0$), fundamental ($n = 0$) inertial–acoustic oscillations as a function of r. The oscillations are assumed to occur isothermally in isothermal disks. The rotation is Keplerian ($\Omega = \Omega_K$) under a pseudo-Newtonian potential and $c_T^2 k^2 = 0.1\Omega_K^2$. The case of the Newtonian potential is also shown for comparison. (After Kato et al. 1998)

disks are bounded with surfaces with no pressure. (This does not represent real situations of accretion flows, but would bring about slight differences in the final results.) The unperturbed flows are assumed to be adiabatic and inviscid. On such disks, oscillations are superposed, which are assumed to occur quasi-adiabatically and quasi-inviscidly.

The necessary tools used to derive the criterion have been prepared by Lynden-Bell and Ostriker (1967). Applying their formalism, Cox and Everson (1983) derived a criterion of the oscillatory instability of disks. In the following, a different form of the criterion is presented by a method somewhat different from that of Cox and Everson (Kato 1991; Kato et al. 1998), including the case of non-axisymmetric oscillations ($m \neq 0$).

The final expression of our present criterion is already given by Kato (1991) without any derivation. Kato et al. (1998), on the other hand, presented a derivation, but restricted it only to the case of axisymmetric perturbations. [The criterion on this latter case is already derived by Kato (1978) by using Eulerian formulations.] Since the procedures shown here are the same as those given by Kato et al. (1998) till a certain stage, we focus mainly on the parts characteristic to non-axisymmetric perturbations.

7.1. Basic Equations and General Stability Criterion

The Lagrangian displacement is denoted by $\boldsymbol{\xi}$, and the Lagrangian changes of other physical quantities are denoted by attaching δ as $\delta\rho$. The equation of continuity describing small-amplitude perturbations is then

$$\delta\rho + \rho_0 \operatorname{div} \boldsymbol{\xi} = 0. \tag{74}$$

The equation of motion describing the perturbations is

$$\frac{D_0^2\boldsymbol{\xi}}{Dt^2} + \delta\left(\frac{1}{\rho}\nabla p + \nabla\psi\right) = \delta\boldsymbol{N}, \tag{75}$$

where D_0/Dt, defined by

$$\frac{D_0}{Dt} = \frac{\partial}{\partial t} + \boldsymbol{u}_0 \cdot \nabla \equiv \frac{\partial}{\partial t} + M, \tag{76}$$

is the Lagrangian time derivative along the unperturbed flow $\boldsymbol{u}_0(\boldsymbol{r}, t)$, and $\partial/\partial t$ and ψ are the Eulerian time derivative and gravitational potential, respectively. The quantity $\boldsymbol{N}$ is the viscous stress force per unit mass. The term $D_0^2\boldsymbol{\xi}/Dt^2$ in equation (75) comes from the fact that the operator δ and D/Dt (the time derivative along the perturbed flow $\boldsymbol{v}$) can be commuted with each other (Lynden-Bell, Ostriker 1967) as

$$\delta\left(\frac{D\boldsymbol{v}}{Dt}\right) = \frac{D_0}{Dt}\delta\boldsymbol{v} = \frac{D_0^2}{Dt^2}\boldsymbol{\xi}. \tag{77}$$

The energy equation describing the perturbations is

$$\frac{D_0}{Dt}\delta p - c_s^2\frac{D_0}{Dt}\delta\rho = \delta\left[(\Gamma_3 - 1)(-\operatorname{div}\boldsymbol{F} + \Phi)\right], \tag{78}$$

where $\boldsymbol{F}$ and Φ are the energy flux and thermal energy generation rate (per unit volume), respectively. In equation (78), Γ_3 is an exponent specifying the ratio of the specific heats in the case when the effects of radiation pressure are taken into account, and c_s is the speed of sound, defined by $c_s^2 = \Gamma_1 p_0/\rho_0$, where Γ_1 is another exponent specifying the ratio of the specific heats.

All perturbed quantities are assumed to be proportional to $\exp(i\omega t)$. Then, expressing $\delta[(1/\rho)\nabla p + \nabla\psi]$ in equation (75) in terms of $\boldsymbol{\xi}$ by using equations (74) and (78), we have after lengthy manipulations (Lynden-Bell, Ostriker 1967; Kato et al. 1998)

$$-\omega^2\boldsymbol{A}(\boldsymbol{\xi}) + \omega\boldsymbol{B}(\boldsymbol{\xi}) + \boldsymbol{C}(\boldsymbol{\xi}) = \rho_0\delta\boldsymbol{N} - \nabla(\delta p)_{\mathrm{na}}, \tag{79}$$

where

$$\boldsymbol{A}(\boldsymbol{\xi}) = \rho_0\boldsymbol{\xi}, \tag{80}$$

$$\boldsymbol{B}(\boldsymbol{\xi}) = 2i\rho_0 M\boldsymbol{\xi}. \tag{81}$$

The expression for $\boldsymbol{C}(\boldsymbol{\xi})$ is omitted here, since it is complicated but unnecessary here (see Lynden-Bell and Ostriker for a detailed expression). The important facts to be noticed here are that $\boldsymbol{A}$, $\boldsymbol{B}$, and $\boldsymbol{C}$ are all Hermitian operators, which means that the quantities a, b, and c defined below are all real (Lynden-Bell, Ostriker 1967):

$$a \equiv \int \boldsymbol{\xi}^* \cdot \boldsymbol{A}(\boldsymbol{\xi})\, d^3r = \int \rho_0\boldsymbol{\xi}^* \cdot \boldsymbol{\xi}\, d^3r, \tag{82}$$

$$b \equiv \int \boldsymbol{\xi}^* \cdot \boldsymbol{B}(\boldsymbol{\xi})\, d^3r = 2i\int \rho_0\boldsymbol{\xi}^* \cdot M\boldsymbol{\xi}\, d^3r, \tag{83}$$

$$c \equiv \int \boldsymbol{\xi}^* \cdot \boldsymbol{C}(\boldsymbol{\xi})\, d^3r, \tag{84}$$

where the asterisk denotes the complex conjugate. To derive these Hermitian properties the surface conditions mentioned before (i.e., the pressure p_0 vanishes on the surface and there is no mass flow crossing the surface) are used. In equation (79), $(\delta p)_{\mathrm{na}}$ is the non-adiabatic part of δp, defined by

$$(\delta p)_{\mathrm{na}} \equiv \delta p - \Gamma_1\frac{p_0}{\rho_0}\delta\rho. \tag{85}$$

The Lagrangian time derivative of $(\delta p)_{\rm na}$ is nothing but the right-hand side of equation (78):

$$\frac{D_0}{Dt}(\delta p)_{\rm na} = \delta[(\Gamma_3 - 1)(-\,{\rm div}\,\boldsymbol{F} + \Phi)]. \tag{86}$$

If equation (79) is multiplied by $\boldsymbol{\xi}^*$ and integrated over the entire volume of the configuration, we obtain

$$-a\omega^2 + b\omega + c = \int \rho_0 \boldsymbol{\xi}^* \cdot \left[\delta \boldsymbol{N} - \frac{1}{\rho_0}\nabla(\delta p)_{\rm na}\right] d^3r, \tag{87}$$

where a, b, and c are all real as mentioned before.

The effects of dissipative (viscous and thermal) processes on the pure time periodic oscillations are taken to be small perturbations. Then, the eigenfrequency ω and the eigenfunction $\boldsymbol{\xi}$ are written as

$$\omega = \omega_0 + \omega_1, \tag{88}$$

$$\boldsymbol{\xi} = \boldsymbol{\xi}_0 + \boldsymbol{\xi}_1, \tag{89}$$

where ω_0 (real) and $\boldsymbol{\xi}_0$ are, respectively, the unperturbed parts of the frequency and eigenfunction, and ω_1 (complex in general) and $\boldsymbol{\xi}_1$ are, respectively, small perturbations over ω_0 and $\boldsymbol{\xi}_0$ by dissipative processes. (In section 6, ω_0 and ω_1 are denoted, respectively, by $\omega^{(0)}$ and $\omega^{(1)}$.)

After substituting equations (88) and (89) into equation (87) we take the linear parts of the resulting equation with respect to dissipative processes. The imaginary part of the equation then gives (Kato et al. 1998)

$$(-2a\omega_0 + b)\Im\omega_1 = \Im\left[\int \rho_0 \boldsymbol{\xi}_0^* \cdot \delta \boldsymbol{N} d^3r - \int \boldsymbol{\xi}_0^* \cdot \nabla(\delta p)_{\rm na}\, d^3r\right]. \tag{90}$$

If the solutions in the limit of inviscid and adiabatic oscillations (i.e., ω_0 and $\boldsymbol{\xi}_0$) are known, we can calculate $\Im\omega_1$ from this equation. The oscillations are overstable if $\Im\omega_1 < 0$. The physical meanings of equation (90) are discussed below.

7.2. *Wave Energy and Growth Rate*

Let us first derive an expression for the wave energy of perturbations. We assume that a weakly and exponentially growing artificial force $\delta \boldsymbol{f}$ (per unit mass) is acting on a disk in the direction parallel to the displacement $\boldsymbol{\xi}$. During the initial epoch ($t = -\infty$) when the force began to work on the perturbation, both of the force and the perturbation are taken to have had negligible amplitudes. After that, by the effects of the force, the perturbation grows. The work done on the perturbation between $t = -\infty$ and $t = t$ should be regarded as the wave energy E of the perturbation at $t = t$. In this sense, the wave energy of perturbations, E, can be written as

$$E = \frac{1}{2}\Re \int_{-\infty}^{t} dt \int \rho_0 \left(\frac{D_0\boldsymbol{\xi}}{Dt}\right)^* \cdot \delta \boldsymbol{f}\, d^3r, \tag{91}$$

where $\Re$ represents the real part. Although $D_0\boldsymbol{\xi}/Dt$ is expressed as $i\omega\boldsymbol{\xi} + (r\Omega \boldsymbol{i}_\varphi \cdot \nabla)\boldsymbol{\xi}$, the terms resulting from $(r\Omega \boldsymbol{i}_\varphi \cdot \nabla)\boldsymbol{\xi}$ vanish when the volume integration of equation (91) is performed.

Since an artificial force $\delta \boldsymbol{f}$ (and thus $\boldsymbol{\xi}$ also) is assumed to have a time-dependence of $\exp(i\omega t)$ with $\omega_i \equiv \Im(\omega) < 0$ (i.e., weakly growing), the time integral of equation (91) is performed to obtain

$$E = -\frac{\omega_0}{4\omega_i}\Im \int \rho_0 (\boldsymbol{\xi}^* \cdot \delta \boldsymbol{f})\, d^3r. \tag{92}$$

Since the artificial force $\delta \boldsymbol{f}$ is working on the right-hand side of equation (75), the integration in equation (92) is nothing but $-a\omega^2 + b\omega + c$ and its imaginary part is $(-2a\omega_0 + b)\omega_i$. Hence, equation (92) shows that the wave energy of perturbations can be written as

$$E = -\frac{1}{4}\omega_0(-2a\omega_0 + b). \tag{93}$$

Equation (90) can thus be expressed as

$$(-\Im\omega_1)E = \frac{\omega_0}{4}\Im\left[\int \rho_0 \boldsymbol{\xi}_0^* \cdot \delta \boldsymbol{N}\, d^3r - \int \boldsymbol{\xi}_0^* \cdot \nabla(\delta p)_{\rm na}\, d^3r\right]. \tag{94}$$

That is, the rate of energy change of perturbations, i.e., $(-\Im\omega_1)E$, is related to the work done both by the viscous force and by the pressure force resulting from non-adiabatic processes.

Next, we write explicitly the wave energy E in terms of the velocity perturbations. The Lagrangian velocity perturbation $\delta \boldsymbol{v}$ is written as $D_0\boldsymbol{\xi}/Dt$. It can also be expressed as $\boldsymbol{u}_1 + (\boldsymbol{\xi} \cdot \nabla)\boldsymbol{u}_0$, where $\boldsymbol{u}_1$ is the Eulerian velocity perturbation over the rotational velocity $\boldsymbol{u}_0$ of the unperturbed state; i.e., $\boldsymbol{u}_0 = \boldsymbol{i}_\varphi r\Omega(r)$. Hence, equating the above two expressions for a Lagrangian velocity perturbation, and after some arrangement we obtain the following relations between $\boldsymbol{\xi}$ and $\boldsymbol{u}(u_r, u_\varphi, u_z)$:

$$i(\omega - m\Omega)\xi_r = u_r, \tag{95}$$

$$i(\omega - m\Omega)\xi_\varphi = u_\varphi + \xi_r r\frac{d\Omega}{dr}, \tag{96}$$

$$i(\omega - m\Omega)\xi_z = u_z. \tag{97}$$

Quantities a and b given by equations (82) and (83) are now expressed in terms of u_r, u_φ, and u_z by using the above relations. We have then, after some manipulations,

$$\begin{aligned}(-2a\omega_0 + b)\omega_0 &= -2\int \frac{1}{\omega_0 - m\Omega}\rho_0(u_r^* u_r + u_z^* u_z)\, d^3r \\ &\quad - \int \frac{1}{\omega_0 - m\Omega}\rho_0 \left\{\left[u_\varphi + \frac{\kappa^2/2\Omega}{i(\omega_0 - m\Omega)}u_r\right]^* \right. \\ &\quad \left. \times \left[u_\varphi + \frac{r d\Omega/dr}{i(\omega_0 - m\Omega)}u_r\right] + {\rm c.c.}\right\} d^3r,\end{aligned} \tag{98}$$

where c.c. denotes the complex conjugate. In geometrically thin disks, the φ-component of equation of motion describing perturbations is written as

$$i(\omega - m\Omega)u_\varphi + \frac{\kappa^2}{2\Omega}u_r = 0. \tag{99}$$

Hence, the second integral on the right-hand side of equation (98) vanishes and we finally have

$$E = \frac{1}{2}\int \frac{\omega_0}{\omega_0 - m\Omega}\rho_0(u_r^* u_r + u_z^* u_z)\, d^3r. \tag{100}$$

This equation clearly shows that inside and outside the corotation radius, which is defined as the radius where $\omega_0 = m\Omega(r)$ holds, the sign of wave energy is changed. Inside the radius the wave energy is negative, while it is positive outside. (This is well known in the density wave theory of galactic dynamics and also in the disk instability theory in relation to the Papaloizou–Pringle instability.) The above formulation also shows that the perturbation method adopted here is invalid when the perturbations have a non-negligible amplitude around the corotation radius, since there is a singularity there.

We next consider the right-hand side of equation (94). By using equations (95)–(97) and equation (99), we can express the first term on the right-hand side of equation (94) in terms of u_r, u_φ, u_z, and N_i. The second term on the right-hand side can be rewritten by performing the integration by part. After these procedures we can write equation (94) as (Kato 1991)

$$\begin{aligned} &2(-\Im\omega_1)\int(\omega_0-m\Omega)^{-1}(u_r^*u_r+u_z^*u_z)d^3r \\ &=\Re\int(\omega_0-m\Omega)^{-1}\rho_0\left(u_r^*N_{r,1}+\frac{4\Omega^2}{\kappa^2}u_\varphi^*N_{\varphi,1}+u_Z^*N_{Z,1}\right)d^3r \\ &+\Re\int(\omega_0-m\Omega)^{-1}\left(\frac{\delta T}{T}\right)^*(-\operatorname{div}\boldsymbol{F}_1+\Phi_1)d^3r, \end{aligned} \tag{101}$$

where $N_{r,1}$, $N_{\varphi,1}$, $N_{z,1}$ are the (Eulerian) r-, φ-, and z-components of viscous stress force (per unit mass), and Φ_1 is the (Eulerian) perturbations of viscous heat generation. Detailed expressions for these quantities are omitted here, since they are lengthy and boring [see, for example, Appendix B of Kato et al. (1998) for detailed expressions]. It is noted that the effects of viscous and heat imbalances in the unperturbed state were neglected in deriving equation (101). That is, we assumed $\delta N \sim N_1$ and $\delta(-\operatorname{div}\boldsymbol{F}+\Phi)\sim(-\operatorname{div}\boldsymbol{F}+\Phi)_1$ (see section 8 for brief comments on effects of imbalances). A general relativistic version of equation (101) with the Kerr metric is given by Kato (1993) under the simplification that the perturbations are local.

As mentioned before, the presence of the term $(\omega_0 - m\Omega)^{-1}$ in the above equation is related to the fact that the wave energy E changes its sign at the corotation radius. In problems treating one-armed oscillations, however, the corotation radius usually occurs outside the oscillating region. In this sense, the criterion (101) can be used, in practice, in studying the stability criterion.

In the limit of no rotation ($\Omega = 0$), the terms resulting from viscous effects in equation (101) vanish and we have

$$\begin{aligned} &2(-\Im\omega_1)\int\rho_0(u_r^*u_r+u_z^*u_z)\,d^3r \\ &\qquad=\Re\int\left(\frac{\delta T}{T}\right)^*(-\operatorname{div}\boldsymbol{F}_1+\epsilon_1)\,d^3r. \end{aligned} \tag{102}$$

This is nothing but the stability criterion (the Eddington criterion) well-known in the theory of stellar pulsation (e.g., Unno et al. 1989). In this equation the term ϵ_1 represents the perturbation of the nuclear energy generation rate by oscillations. [This term should be included in equation (101), but has been neglected since nuclear energy generation is negligible, except for special cases, compared with viscous heat generation in accretion disks.]

Equation (101) clearly demonstrates that viscosity has two effects on excitation of oscillations. One is a thermal process (process [1]), being represented by Φ_1 in equation (101). This is a counterpart of the ϵ-mechanism. The other one is a dynamical process (process [2]), and is represented as the first integral on the right-hand side of equation (101). This dynamical process of viscosity is characteristic of the accretion disk oscillations, as mentioned before.

7.3. *On the Viscous Excitation of Some Basic Modes*

In subsection 6.1 we have demonstrated that the fundamental inertial–acoustic oscillations ($n = 0$) can be excited by process [2]. Here we show that the instability by process [2] is related to $u_\varphi^* N_{\varphi,1}$ becoming positive and discuss the physical meaning of $u_\varphi^* N_{\varphi,1} > 0$. Next, we discuss the sign of $u_\varphi^* N_{\varphi,1}$ for some other oscillation modes and possibilities of their excitation.

The azimuthal component of Lagrangian variation of velocity, δv_φ, is expressed as

$$\delta v_\varphi = u_\varphi + (\boldsymbol{\xi}\cdot\nabla\boldsymbol{u}_0)_\varphi = u_\varphi + \xi_r\frac{d}{dr}(r\Omega). \tag{103}$$

Furthermore, the combination of equation of (95) and (99) gives

$$\xi_r = -\frac{2\Omega}{\kappa^2}u_\varphi. \tag{104}$$

Hence, from the above two relations we have

$$\delta v_\varphi = \frac{2\Omega^2}{\kappa^2}u_\varphi. \tag{105}$$

On the other hand, the change in the azimuthal component of the viscous force (per unit mass) due to perturbations is $\delta\boldsymbol{N}(\sim\boldsymbol{N}_1)$. Hence, the rate of work done (per unit mass) on oscillations by the viscous force in the azimuthal direction is $(2\Omega^2/\kappa^2)u_\varphi^* N_{1\varphi}$. This is a part of the origin of the second term in the first integration on the right-hand side of equation (101). If this term is positive, positive work is done on oscillations, and it contributes to excitation of the oscillations.

Since the φ-component of the viscous force is given by

$$N_\varphi = \frac{1}{\rho r^2}\frac{\partial}{\partial r}\left[r^3\eta\frac{\partial}{\partial r}\left(\frac{v_\varphi}{r}\right)\right], \tag{106}$$

we have

$$N_{\varphi,1} = -\frac{\eta_0}{\rho_0}k^2u_\varphi - ik\frac{\eta_0}{\rho_0}r\frac{d\Omega}{dr}\frac{\eta_1}{\eta_0}, \tag{107}$$

if a local perturbation in the radial direction is considered. When $\eta = \alpha\rho c_s^2/\Omega$ is adopted even in the perturbed state, we have $\eta_1/\eta_0 = p_1/p_0$. In the case of local adiabatic perturbations, the r- and φ-components of equation of motion are, respectively,

$$i(\omega - m\Omega)u_r - 2\Omega u_\varphi = ik\frac{p_1}{\rho_0} \tag{108}$$

and

$$i(\omega - m\Omega)u_\varphi + \frac{\kappa^2}{2\Omega}u_r = 0. \tag{109}$$

Hence, elimination of u_r from these equations gives a relation between p_1/ρ_0 and u_φ:

$$\frac{p_1}{\rho_0} = -i\frac{2\Omega}{k\kappa^2}\left[(\omega - m\Omega)^2 - \kappa^2\right]u_\varphi. \quad (110)$$

Substituting this relation into equation (107), we find that $N_{\varphi,1}$ and u_φ are related by

$$N_{\varphi,1} = -\frac{\eta_0}{\rho_0}k^2\left[1 + \frac{2\Omega^2}{\kappa^2}\frac{d\ln\Omega}{d\ln r}\frac{(\omega - m\Omega)^2 - \kappa^2}{k^2c_{\rm T}^2}\right]u_\varphi, \quad (111)$$

where $c_{\rm T}$ is the isothermal sound speed. That is, $N_{\varphi,1}$ is in phase with u_φ when

$$1 + \frac{2\Omega^2}{\kappa^2}\frac{d\ln\Omega}{d\ln r}\frac{(\omega - m\Omega)^2 - \kappa^2}{k^2c_{\rm T}^2} < 0. \quad (112)$$

If the second term in the brackets of equation (111) are neglected, we have $u_\varphi^* N_{\varphi,1} = -(\eta_0/\rho_0)k^2(u_\varphi^* u_\varphi)$. This is negative and proportional to k^2, representing a part of the usual viscous damping processes in non-rotating systems. The second term in the brackets is related to rotation and is the term of our concern. For oscillations to be excited, $N_{\varphi,1}$ and u_φ must be in phase ($u_\varphi^* N_{\varphi,1} > 0$), since the other terms ($u_r^* N_{r,1}$ and $u_z^* N_{z,1}$) in the first integral of equation (101) are always negative and contribute only to the damping of the oscillations.

(a) Fundamental inertial–acoustic oscillations (n = 0)

In this case $N_{\varphi,1}$ is reduced to

$$N_{\varphi,1} = -\frac{\eta_0}{\rho_0}k^2\left[1 + \frac{2\Omega^2}{\kappa^2}\frac{d\ln\Omega}{d\ln r}\right]u_\varphi, \quad (113)$$

when local perturbations are considered, since $(\omega - m\Omega)^2 - \kappa^2 \sim k^2c_{\rm s}^2$. That is, $u_\varphi^* N_{\varphi,1}$ can certainly become positive. If this positive value can overcome the negative value of $u_r^* N_{r,1}$ [$u_z^* N_{z,1}$ nearly vanishes in the present case of no node in the vertical direction ($n = 0$)], the first integral of equation (101) is positive and the viscosity contributes in net to the excitation of oscillations. This is the case shown in the previous section.

Actually, in the case discussed in section 6 we have

$$N_{r,1} = -\frac{4}{3}\eta_0 k^2 u_r, \quad (114)$$

$$u_\varphi^* u_\varphi = \frac{\kappa^4}{4\Omega^2(\kappa^2 + c_{\rm T}^2k^2)}u_r^* u_r. \quad (115)$$

These give us

$$u_r^* N_{r,1} + \frac{4\Omega^2}{\kappa^2}u_\varphi^* N_{\varphi,1} = -\frac{2\eta_0}{\rho_0}k^2\left[\frac{2}{3} + \frac{\Omega^2}{\kappa^2 + c_{\rm T}^2k^2}\left(\frac{d\ln\Omega}{d\ln r} + \frac{\kappa^2}{2\Omega^2}\right)\right](u_r^* u_r). \quad (116)$$

Substitution of this equation into equation (101) gives the same growth rate as equation (73).

The results of numerical simulations that inertial–acoustic oscillations are generated in the innermost region of relativistic disks (see subsection 5.1) would be due to this excitation mechanism. The excitation of an eccentric deformation ($n = 0$, $m = 1$) of Be star disks would also be due to this mechanism (see subsubsection 4.1.1).

(b) g-mode oscillations

In the case of g-mode oscillations, $(\omega - m\Omega)^2 - \kappa^2 < 0$. Hence, the value in the brackets of equation (111) is always positive and we have $u_\varphi^* N_{\varphi,1} < 0$. That is, the phase relation between $N_{\varphi,1}$ and u_φ always acts so as to dampen the oscillations, distinct from the case of (a). Since all terms of $u_\varphi^* N_{\varphi,1}$, $u_r^* N_{r,1}$, and $u_z^* N_{z,1}$ are negative, the dynamical effects of viscosity (process [2]) always act in the direction to dampen the oscillations (cf., Nowak, Wagoner 1992; Ortega-Rodriguez, Wagoner 2000).

These results show that to excite the g-mode oscillations, some other processes are necessary. One of the possible processes would be the dynamical actions of turbulence (Goldreich, Keeley 1977), which is known as the excitation process of solar oscillations, and is suggested to also be a possible source of excitation of disk oscillations (Nowak, Wagoner 1993).

(c) c-mode oscillations

In the c-mode oscillations, $(\omega - m\Omega)^2 - \kappa^2 > 0$. Hence, as in the case of p-mode oscillations, the value in the brackets of equation (111) can become negative. That is, the phase relation between $N_{\varphi,1}$ and u_φ can act so as to amplify the oscillations. Distinct from the case of (a), however, u_z and $N_{z,1}$ are non-negligible in the present case, and we have $u_z^* N_{z,1} < 0$. The problem to be examined here is thus whether the excitation process by $u_\varphi^* N_{\varphi,1} > 0$ has a sufficient amount to overcome the damping processes by $u_r^* N_{r,1} < 0$ and $u_z^* N_{z,1} < 0$. We cannot have a definite conclusion on this problem until we have detailed informations on eigenvalues and eigenfunctions of the c-mode oscillations. Calculations based on local approximations, however, suggest that the excitation of c-mode oscillations by $u_\varphi^* N_{\varphi,1} > 0$ against the dampings by $u_r^* N_{r,1} < 0$ and $u_z N_{z,1} < 0$ is difficult, although the innermost region of relativistic disks is a favorable place for the excitation (Kato 1993). See Ortega-Rodriguez and Wagoner (2000) for careful studies in the case of Newtonian disks.

Comparisons of expressions for $N_{r,1}$, $N_{\varphi,1}$, and $N_{z,1}$, however, suggest that the c-mode oscillations can be excited in the innermost region of disks, if the viscosity is anisotropic in such a sense that $t_{zz}, t_{rz}, t_{\varphi z} \ll t_{rr}, t_{\varphi\varphi}, t_{r\varphi}$. This kind of anisotropy of the turbulent stress tensor is theoretically expected in accretion-disk turbulence (e.g., Kato, Yoshizawa 1997). The importance of anisotropic turbulence on the excitation of the oscillations has already been suggested by Nowak and Wagoner (1993).

It is noted that c-mode oscillations and warp motions due to viscosity (e.g., Papaloizou, Pringle 1983) are different from each other. In the c-mode oscillations, the pressure makes the warp motions coherent, while in the latter warps the motions become coherent due to the effects of viscosity. Furthermore, in the latter warps viscosity always acts to dampen them, while this is not always the case in the c-mode oscillations. The latter warps are known to be excited by a reaction due to the re-emission of irradiation from the central object (self-irradiated destabilization) (Pringle 1996 and subsequent papers). It would be natural to suppose that the c-mode oscillations are also excited by the same mechanism, when the central object is a neutron star.

Possible excitation mechanisms of various oscillation modes discussed here are briefly summarized in table 4 (see section 9).

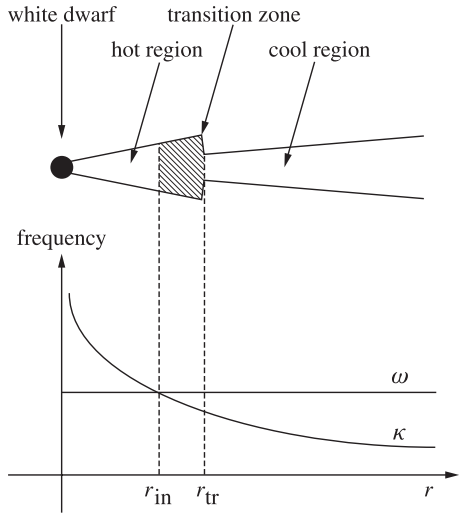

Fig. 13. Schematic picture showing a trapped oscillation on dwarf-novae accretion disks in the outburst stage. A wave whose frequency is ω cannot propagate inside radius r_{in}, since $\omega < \kappa$ there. It also cannot propagate outside radius r_{tr} since the disk thickness changes there sharply. Because of these situations, the wave is trapped in the region hatched in the upper panel. (After Yamasaki et al. 1995)

8. Miscellaneous Issues of Trapping and Excitation

Before closing the main parts of this article, we discuss some issues which have not been considered so far.

(1) Trapped Oscillations Related to a Disk Transition

The trapped oscillations discussed in section 5 are those resulting from a non-monotonic spatial distribution of epicyclic frequency $\kappa(r)$ in relativistic disks. In addition to these kinds of trapped oscillations, we can expect another types of trapped oscillations, which are realized even in the Newtonian disks. Two possible examples are presented here:

(a) The dwarf nova activity is now understood based on the disk instability model (see reviews by Osaki et al. 1993; Osaki 1996). This model says that in the stage of outbursts the dwarf nova disks, which are non-relativistic Keplerian, undergo limit-cycle oscillations because of the thermal instability. This instability brings about a transition front separating hotter and colder disks. Let us now consider the situation in which an inner geometrically thicker hot disk touches at r_{tr} an outer geometrically thiner cold disk, and that an axisymmetric p-mode wave with no node in the vertical direction ($n = 0$) exists in the region of $r < r_{tr}$. The wave frequency ω is higher than the epicyclic frequency at r_{tr}.

The wave propagates outward on the inner geometrically thicker disk, but will be reflected back inward at the transition radius r_{tr}, since the disk thickness sharply changes there and practically there is no gas outside r_{tr} except for the equatorial region. The reflected wave, however, will be reflected back outward at the radius (say r_{in} where the epicyclic frequency κ becomes equal to the wave frequency ω), since inside the radius the wave cannot propagate there. This means that the oscillations with $\omega \sim \kappa(r_{in})$ will be trapped in the region between r_{in} and r_{tr}, as demonstrated in figure 13. Eigenfunctions of this type of trapped oscillations were studied by Yamasaki et al. (1995) in order to explain QPOs observed in some dwarf novae. Their analyses show that these oscillations can be excited by the κ-mechanism (Yamasaki, Kato 1996).

(b) Another type of trapped oscillations is expected in the transition region between an advection-dominated accretion flow (ADAF) and a standard Shakura–Sunyaev disk (SSD). The advection-dominated accretion flows around compact objects have been extensively studied in recent years, since such flows can explain well the spectra of the hard state of X-ray stars and of the low-luminosity galactic nuclei (see a review by Narayan et al. 1998). The accretion disks generally cannot be ADAFs from their outermost region, unless they start from the beginning with a hot virial temperature. That is, there must be a transition from an outer SSD to an inner ADAF. There is, however, no widely recognized model of the transition region. One of the possible models is that the transition occurs in a radially narrow region (Honma 1996; Manmoto, Kato 2000). In this transition model, the pressure decreases sharply inwards in a narrow transition region. This sharp pressure decrease is accompanied by a much sharper inward decrease in density, although the temperature increases inward.

One of important characteristics of this transition is that a super-Keplerian rotation is realized in the transition region (Honma 1996; Abramowicz et al. 1998). In the ADAF region the disk rotation is sub-Keplerian, but it becomes super-Keplerian in the transition region and sharply decreases in the outer boundary of the transition region to join the Keplerian rotation in the SSD region. Since a super-Keplerian rotation changes to a Keplerian one in a narrow region, the specific angular momentum also sharply decreases outward in this narrow region. An outward decrease of specific angular momentum leads to the Rayleigh instability of disks if the stabilizing effects due to the inhomogeneity of the region is negligible. In the present problem, however, the physical quantities, such as density, are sharply change in this region, which acts against the onset of the Rayleigh instability.

If this latter action against the Rayleigh instability is stronger, perturbations in the region are oscillations rather than growing motions. Furthermore, the frequency of the oscillations would be low if the above two actions acting in the opposite directions are close to each other and are almost cancelled out. An important point is that such low frequency oscillations will be trapped in the narrow transition region by the following reasons. In the surrounding regions of the transition region (i.e., the regions of ADAF and SSD), the spatial changes of the physical quantities are not sharp. Hence, the propagation behavior of perturbations in the surrounding regions is governed by the relation between the epicyclic frequency κ and the wave frequency ω. Since the waves considering here have frequencies much smaller than κ in the surrounding media, the waves can not propagate in these regions. This means that the waves are trapped in the narrow boundary region of the transition region. This possibility has been studied by Kato and Manmoto (2000) under the expectation that trapped oscillations explain the 1–15 Hz quasi-periodic oscillations observed in the microquasar GRS 1915+105 (Markwardt et al. 1999).

In Honma's model, the region where the oscillations are trapped are narrow. Hence, one may suppose that such trapped oscillations cannot cause luminosity variations of the observable amount. This is, however, not the case, since the transition region emits a comparable amount of radiation with the whole luminosity emitted in the SSD region (Honma 1996; Kato, Nakamura 1998; Manmoto, Kato 2000).

Finally, it is noted that the presence of trapped oscillations in the transition layer between ADAF and SSD is based on the assumption that the transition occurs in a sharp narrow region. For this to be realized, a large (turbulent) conductivity is necessary. It is not yet clear whether such a large (turbulent) conductivity is expected in real disks (cf. Abramowicz et al. 2000).

(2) Time Lag of Viscous Responses

The form of viscosity has crucial effects on excitation of oscillations. Roughly speaking, an increase (decrease) of the viscosity in the compressed (expanded) phase acts in favor of oscillation amplification.

So far, we have adopted a diffusion-type viscous force with the so-called α-model of turbulent viscosity. A diffusion-type viscous force, however, does not always represent real situations. This is because a basic assumption involved in the diffusion approximation is that the turbulence responds instantly to a change in the environment. In other words, any information is transported with an infinite speed. This unphysicalness becomes prominent as an violation of causality when the transonic flows beyond the inner edge of accretion flows are treated (Pringle 1977). To resolve this problem, many attempts to improve the expression for the viscous force have been made (Popham, Narayan 1992; Narayan 1992; Narayan et al. 1994; Kato, Inagaki 1994; Kato 1994a; Papaloizou, Szuszkiewicz 1994).

When we consider the effects of viscous forces on oscillations, the drawback of the diffusion-type viscous force again becomes noticeable, although we adopted its expression so far. The time scale of the turbulence will generally of the order of $1/\Omega$, which is comparable to the dynamical timescale in disks. This means that when we treat oscillations whose frequencies are much lower than Ω, the adoption of a diffusion-type viscous force will be appropriate as long as it is a good description of the viscous stress force in steady disks. In the opposite case, where the frequency of oscillations is higher than that of turbulent motions, the turbulence cannot respond instantly to a time change of the medium. In other words, we must consider a time lag of turbulence in response to the oscillations.

To study the effects of the time lag of the response of the turbulent viscous stress force on oscillatory motions, an evaluation of the turbulent viscous stress tensor based on a second-order closure modeling (Kato 1994a) is appropriate, since the time lag in the response of the turbulence is taken into account automatically in the modeling. Kato (1994b) (see also Yamasaki, Kato 1996) applied this seconder-order closure modeling of turbulence to stydying excitation of disk oscillations. The results actually show, as expected, that the time lag of the response of turbulence acts in a direction so as to stabilize the oscillations.

As is well known, there is yet no established theory of turbulence describing inhomogeneous time-dependent turbulent flows. Hence, our understanding on the excitation of oscillations on disks by turbulent viscosity is still far from a satisfactory stage.

(3) Effects on Oscillations of Viscosity and Thermal Imbalance in the Unperturbed State

So far, we have neglected the effects on oscillations of the presence of viscosity in the unperturbed state. The presence of viscosity introduces large scale circulations as well as accretion flows in the unperturbed state. The effects of these flows on oscillations have been neglected in the analyses of sections 6 and 7. In the case of local oscillations, their effects on oscillations will be generally only to change the eigenfrequency to a Doppler-shifted one, and there will be no essential change on growth rate. See Ortega-Rodriguez and Wagoner (2000) for a full examination of the effects of viscosity on disk oscillations within the framework of a perturbation theory.

The effects of a thermal imbalance in the unperturbed state are also neglected in our analyses. That is, $\delta[-\mathrm{div}\,\boldsymbol{F}+\Phi]$ is approximated to be $[-\mathrm{div}\,\boldsymbol{F}+\Phi]_1$. The effects of $[-\mathrm{div}\,\boldsymbol{F}+\Phi]_0 \neq 0$ on oscillations, however, will not always negligible on stability of oscillations. In advection-dominated disks, the thermal energy generated by viscosity is not radiated away locally, i.e., it is transported inward as internal energy. That is, $[-\mathrm{div}\,\boldsymbol{F}+\Phi]_0 \neq 0$. A careful examination of the effects of this thermal imbalance on excitation of disk oscillations should be made.

Here, we comment on stellar pulsational instability resulting from a thermal imbalance. The pre–main-sequence stars are in thermal imbalance. That is, the radiative loss is maintained by a release of gravitational energy by contraction. These pre–main-sequence stars are found to be pulsationally unstable by thermal imbalance (Kato, Unno 1966; Okamoto 1967). A detailed formulation of stability criterion of stars, including the effects of thermal imbalance, has been made by a series of papers by Cox and his collaborators (e.g., Aizenman, Cox 1975). Their procedure will be generalized in order to study the stability criterion of a disk in a thermal imbalance.

9. Brief Summary

In this paper we have reviewed two issues concerning disk oscillations. The first one are characteristics of disk oscillations, while focusing on large-scale oscillation modes and trapped oscillations. The second one is the excitation mechanisms of disk oscillations.

The reasons why we have restricted our attention to trapped oscillations and oscillations with large-scale patterns are that, except for these oscillations, disk oscillations would not bring about any large-amplitude luminosity variations to observers outside the disks. That is, in other type of oscillations, various parts of a disk oscillate with different phases, the superposition of which leads to a cancellation of the variations.

From the viewpoint of a global pattern, one-armed ($m = 1$) oscillations are particularly interesting. They are also low-frequency oscillations, except for some limiting cases. The one-armed oscillations of $n = 0$ are rotations of eccentric deformations of the disk plane. These oscillations have been applied

Table 1. Low-frequency oscillation modes on Newtonian Keplerian disks.*

Mode	Angular frequency	Numerical value (Hz)	Section
Eccentric $(n,m)=(0,1)$			
Pressure deformation	$-\Omega(k_r c_s/\Omega)^2$	$\sim 4.0\times10^{-5}x^{-3/2}m^{1/2}\lambda_{10}^{-2}$	4.1.1
Tidal deformation	$\Omega(r/a)^3(M_2/M)$	$\sim 9.6\times10^{-7}x^{-3/2}m^{1/2}$	4.1.2
Corrugation $(n,m)=(1,1)$	$\pm k_r c_s$	$\sim 6.3\times10^{-5}x^{-3/2}m^{1/2}\lambda_{10}^{-1}$	4.2

* $x\equiv r/r_\odot$, $m\equiv M/M_\odot$, $\lambda_{10}\equiv\lambda/10H$ (λ is radial wavelength).

Table 2. Trapped oscillations on relativistic Keplerian disks.*

Mode	Trapped region	Angular frequency	Numerical value (Hz)	Section
p-mode $(n,m)=(0,0)$	$\sim r_{\max}$	$\sim\kappa_{\max}$		
Schwarzschild BH			$\sim 7.1\times10^{2}m^{-1}$	5.1
Extreme Kerr			$\sim 2.3\times10^{3}m^{-1}$	5.1
g-mode $(n,m)=(1,0)$	$\sim r_{\max}$	$\sim\kappa_{\max}$		
Schwarzschild BH			$\sim 7.1\times10^{2}m^{-1}$	5.2
Extreme Kerr			$\sim 2.3\times10^{3}m^{-1}$	5.2
c-mode $(n,m)=(1,1)$	inner region			
Schwarzschild BH	wide	$\ll\kappa_{\max}$	$\sim 4.0\times10^{-5}x^{-3/2}m^{1/2}\lambda_{10}^{-2}$	4.2 and 5.3
Extreme Kerr	very narrow	$>\kappa_{\max}$		5.3

* $x\equiv r/r_\odot$, $m\equiv M/M_\odot$, $\lambda_{10}\equiv\lambda/10H$ (λ is radial wavelength).

Table 3. Trapped oscillations related to disk transition.

Disk	Trapped region	Angular frequency	Numerical value (Hz)	Section
An outburst stage	$r_{\rm in}-r_{\rm tr}$	$\sim\kappa_{\rm in}$	$\sim 6.3\times10^{-4}x_{\rm in}^{-3/2}m^{1/2}$	8(1a)
ADAF+SSD	$\sim r_{\rm tr}$	$\ll\kappa_{\rm tr}$		8(1b)

Table 4. Excitation mechanisms of disk oscillations.

Disk	Mode	Excitation mechanism	Section
Newtonian	Eccentric $(n,m)=(0,1)$		
	Pressure deformation	Turbulent viscosity	7.3
	Tidal deformation	Tidal instability	4.1.2
Relativistic	p-modes $(n,m)=(0,0)$	Turbulent viscosity	6.1 and 7.3
	g-modes $(n,m)=(1,0)$	Dynamical action of turbulence ?	7.3
	c-modes $(n,m)=(1,1)$	Turbulent viscosity ?	7.3
		or Self-irradiation ?	7.3

to explain the V/R variations in Be stars [see Okazaki (2000) for recent progress] and superhump phenomena of dwarf novae (Osaki 1985). One-armed ($m=1$) inertial–acoustic modes of $n=1$ (i.e., corrugation waves) are global, low-frequency tilt motions when the central source is a slow rotator ($a\ll1$). If the central source is a rapid rotator, however, the c-mode oscillations are no longer low-frequency global motions (Silbergleit et al. 2000).

Some of axisymmetric oscillations are interesting, since they become trapped oscillations when the disk is relativistic. In relativistic disks the radial distribution of the epicyclic frequency $\kappa(r)$ is no longer monotonic and there is a maximum, say $\kappa_{\max}$, at a radius, of $r_{\max}$. Because of the presence of $\kappa_{\max}$, the fundamental p-mode ($n=0$, $m=0$) and the fundamental g-mode ($n=1$, $m=0$) are trapped in the inner region around $r_{\max}$ with frequencies of $\sim\kappa_{\max}$ in different contexts. The 67-Hz QPOs observed in GRS 1915+105 are considered to be attributed to the g-mode oscillations (Nowak et al. 1997).

In tables 1 and 2 we summarize the basic properties of disk oscillations. Table 1 is for low-frequency oscillations on Newtonian Keplerian disks. Table 2 is for trapped oscillations on relativistic disks. It is noted that the corrugation waves are no longer low-frequency oscillations when the spin parameter a is not small. In section 8 we have discussed some possible trapped oscillations resulting from the transition region connecting a colder disk to a hotter one. The results are summarized in table 3.

The second subject which we discussed was the excitation processes of disk oscillations. The excitation processes of disk oscillations are rather different from those of stellar oscillations in the sense that viscous processes are important in disk oscillations, although they are quite minor in stellar oscillations. The results of our analyses show that some of the important oscillation modes in disks can be excited by visous processes of turbulence. It should be noted, however, that the nature of the turbulence in disks is not yet well understood. Hence, there

are still ambiguities concerning a quantitative estimate of the growth or damping rate of oscillations. Possible excitation processes of some of the basic oscillation modes considered in this paper are summarized in table 4.

There are some issues which are not discussed in this article. For example, large-scale non-axisymmetric oscillations are of interest in the viewpoint of angular momentum transport in disks (Vishniac, Diamond 1989), which was, however, not discussed in this paper. In our analyses the disks are assumed to be in a convectively neutral state, i.e., $N_r^2 = N_z^2 = 0$. This is, however, not always the case. Especially, $N_z^2 \neq 0$ brings about non-negligible modifications on the characteristics of the g-mode oscillations (e.g., Hirotani, Kato 1995).

Since our attention in this paper was mainly on relatively large-scale oscillations on geometrically thin disks, the effects of a vertical variation of the angular velocity of rotation was neglected. The effects of the variation, however, will not be negligible when oscillations in geometrically thick disks are considered. The instabilities on disks are of importance in relation to wave phenomena on disks. For example, the Papaloizou–Pringle instability (e.g., Papaloizou, Pringle 1985) and the Rossby wave instability (e.g., Li et al. 2000) are related to wave phenomena. These instability problems were, however, not discussed here.

Finally, we mention that we have completely neglected in this review the effects of magnetic fields on oscillations, except that we regarded turbulent magnetic fields as the main source of viscosity. Magnetic fields, however, introduce many wave phenomena as well as instabilities, related to disk activities. In this sense the magnetic field is one of the most important ingredients to understand the time variabilities of disks. The subjects concerning magnetic fields are, however, outside of this paper, since they are related widely and deeply to many other fields and beyond the scope of this review.

The author thanks many colleagues for discussions on various aspects of accretion disks. For disk oscillations, he is especially indebted to J. Fukue, F. Honma, R. Matsumoto, S. Mineshige, M. Nowak, A. T. Okazaki, R. Taam, and R. Wagoner. He thanks S. Mineshige for many invaluable suggestions on the original manuscript, by which the presentation of this article is much improved.

List of Symbols

Symbol	Meaning
(r, φ, z)	cylindrical coordinates
$\boldsymbol{F}$	energy flux
G	gravitational constant
H	disk half-thickness
M	mass
M_2	mass of companion star
$M_\odot$	solar mass
$\boldsymbol{N} = (N_r, N_\varphi, N_z)$	viscous force per unit mass
$\boldsymbol{N}_1 = (N_{r,1}, N_{\varphi,1}, N_{z,1})$	Eulerian perturbations of viscous force
N_r, N_z	Brunt–Väisälä frequency (radial/vertical)
$a = cJ/GM^2$	normalized black-hole spin parameter
c	speed of light
c_s	sound speed
c_T	isothermal sound speed
d	binary separation
$\boldsymbol{g} = (-g_r, 0, -g_z)$	gravitational acceleration
$\boldsymbol{g}_\mathrm{eff}$	effective gravitational acceleration
$h_1 = p_1/\rho_0$	pressure perturbation normalized by ρ_0
$\boldsymbol{k} = (k_r, k_\varphi, k_z)$	wavenumber of perturbations
m	number of nodes in the φ-direction
n	number of nodes in the vertical direction
p	pressure
p_0, p_1	unperturbed and Eulerian variations of pressure
r	radius
r_g	Schwarzschild radius
r_max	radius of κ_max
$\hat{r} = r/(r_\mathrm{g}/2)$	normalized radius
t_{ij}	viscous stress tensor
$t_{ij,1}$	Eulerian variation of viscous stress tensor t_{ij}
$t_{r\varphi}$	$r\varphi$-component of t_{ij}
$\boldsymbol{u} = (u_r, u_\varphi, u_z)$	Eulerian variation of velocity by perturbations
$\boldsymbol{v} = (v_r, v_\varphi, v_z)$	velocity
Φ	viscous dissipation function
Ω	angular velocity of rotation
Ω_K	angular velocity of Keplerian rotation
$\Omega_\perp$	frequency of vertical oscillations
α	viscosity parameter
γ	specific heat ratio, adiabatic index
δ	Lagrangian variation
η	dynamical viscosity
$\eta = z/H$	dimensionless vertical coordinates
κ	epicyclic frequency
κ_max	maximum of epicyclic frequency
$\nu = \eta/\rho$	kinematic viscosity
$\boldsymbol{\xi} = (\xi_r, \xi_\varphi, \xi_z)$	Lagrangian displacement
ρ	density
ρ_0, ρ_1	unperturbed and perturbed density
φ	azimuthal angle
$\psi < 0$	gravitational potential
ω	angular frequency of waves
$\tilde{\omega} = \omega - m\Omega$	angular frequency of waves

References

Abramowicz, M. A., Bjornsson, G., & Igumenshchev, I. V. 2000, PASJ, 52, 295
Abramowicz, M. A., Igumenshchev, I. V., & Lasota, J.-P. 1998, MNRAS, 293, 443
Aizenman, M. L., & Cox, J. P. 1975, ApJ, 195, 175
Blumenthal, G. R., Yang, L. T., & Lin, D. N. C. 1984, ApJ, 287, 774
Chen, X., & Taam, R. E. 1995, ApJ, 441, 354
Copeland, J. A., & Heard, J. F. 1963, Publ. David Dunlap Obs., 2, 317
Cowling, T. G. 1957, Magnetohydrodynamics (New York: Interscience Publ.), ch.4
Cox, J. P. 1980, Theory of Stellar Pulsation (Princeton: Princeton University Press)
Cox, J. P., & Everson, B. L. 1983, ApJS, 52, 451
Goldreich, P., & Keeley, D. A. 1977, ApJ, 212, 243
Hines, C. O. 1960, Can. J. Phys., 38, 1441
Hirata, R., & Hubert-Delplace, A.-M. 1981, in Workshop on Pulsating B Stars, eds. M. Auvergne et al. (Nice: Observatoire de Nice), 217
Hirose, M., & Osaki, Y. 1990, PASJ, 42, 135
Hirose, M., & Osaki, Y. 1993, PASJ, 45, 595
Hirotani, K., & Kato, S. 1995, PASJ, 47, 645
Honma, F. 1996, PASJ, 48, 77
Honma, F., Matsumoto, R., & Kato, S. 1992, PASJ, 44, 529
Ipser, J. R. 1994, ApJ, 435, 767
Ipser, J. R. 1996, ApJ, 458, 508
Kato, S. 1978, MNRAS, 185, 629
Kato, S. 1983, PASJ, 35, 249
Kato, S. 1989, PASJ, 41, 745
Kato, S. 1990, PASJ, 42, 99
Kato, S. 1991, PASJ, 43, 557
Kato, S. 1993, PASJ, 45, 219
Kato, S. 1994a, PASJ, 46, 415
Kato, S. 1994b, PASJ, 46, 589
Kato, S., & Fukue, J. 1980, PASJ, 32, 377
Kato, S., Fukue, J., & Mineshige, S. 1998, Black-Hole Accretion Disks (Kyoto: Kyoto Univ. Press)
Kato, S., Honma, F., & Matsumoto, R. 1988a, MNRAS, 231, 37
Kato, S., Honma, F., & Matsumoto, R. 1988b, PASJ, 40, 709
Kato, S., & Inagaki, S. 1994, PASJ, 46, 289
Kato, S., & Manmoto, T. 2000, ApJ, 541, 889
Kato, S., & Nakamura, K. E. 1998, PASJ, 50, 559
Kato, S., & Unno, W. 1966, PASJ, 19, 1
Kato, S., & Yoshizawa, A. 1997, PASJ, 49, 213
Li, H., Finn, J. M., Lovelace, R. V. E., & Colgate, S. A. 2000, ApJ, 533, 1023
Lin, C. C., & Shu, F. H. 1964, ApJ, 140, 646
Lubow, S. H. 1991, ApJ, 381, 259
Lynden-Bel, D., & Ostriker, J. P. 1967, MNRAS, 136, 293
Maloney, P. R., & Begelman, M. C. 1997, ApJ, 491, L43
Manmoto, T., & Kato, S. 2000, ApJ, 538, 295
Manmoto, T., Takeuchi, M., Mineshige, S., Kato, S., & Matsumoto, R. 1996, in Physics of Accretion Disks, eds. S. Kato, S. Inagaki, S. Mineshige, & J. Fukue (Amsterdam: Gordon and Breach), 57
Markovic, D., & Lamb, F. K. 1999, ApJ, 507, 316
Markwardt, C. B., Swank, J. H., & Taam, R. E. 1999, ApJ, 513, L37
Matsumoto, R., Kato, S., & Honma, F. 1988, in Physics of Neutron Stars and Black Holes, ed. Y. Tanaka (Tokyo: Universal Academy Press), 155
Matsumoto, R., Kato, S., & Honma, F. 1989, in Theory of Accretion Disks, ed. F. Meyer, W. J. Duschl, J. Frank, & E. Meyer-Hofmeister (Dordrecht: Kluwer Academic Publisher), 167
Milsom, J. A., & Taam, R. E. 1997, MNRAS, 286, 358
Miyoshi, M., Morgan, J., Herrnstein, J., Greenhill, L., Nakai, N., Diamond, P., & Inoue, M. 1995, Nature, 373, 127
Morgan, E. H., Remillard, R. A., & Greiner, J. 1997, ApJ, 482, 993
Narayan, R. 1992, ApJ, 394, 261
Narayan, R., Loeb, A., & Kumar, P. 1994, ApJ, 431, 359
Narayan, R., Mahadevan, R., & Quataert, E. 1998, in Theory of Black Hole Accretion Discs, ed. M. A. Abramowicz, G. Bjornsson, & J. E. Pringle (Cambridge: Cambridge Univ. Press), 148
Negueruela, I., Okazaki, A. T., Fabregat, J., Coe, M. J., Munari, U., & Tomov, T. 2000, A&A, submitted
Nelson, R. W., & Tremaine, S. 1995, MNRAS, 275, 897
Nowak, M. A., & Lehr, D. E. 1998, in Theory of Black Hole Accretion Disks, ed. M. A. Abramowicz, G. Bjornsson, & J. E. Pringle (Cambridge: Cambridge Univ. Press), 233
Nowak, M. A., & Wagoner, R. V. 1992, ApJ, 393, 697
Nowak, M. A., & Wagoner, R. V. 1993, ApJ, 418, 187
Nowak, M. A., Wagoner, R. V., Begelman, M. C., & Lehr, D. E. 1997, ApJ, 477, L91
Ogilvie, G. I. 1999, MNRAS, 304, 557
Okamoto, I. 1967, PASJ, 19, 384
Okazaki, A. T. 1991, PASJ, 43, 75
Okazaki, A. T. 1996, PASJ, 48, 305
Okazaki, A. T. 2000, in IAU Colloq. 175, On the Be Phenomenon in Early-Type Stars, eds. M. Smith, H. Henrichs., & J. Fabregat ASP Conf. Ser., 214, 409
Okazaki, A. T., & Kato, S. 1985, PASJ, 37, 683
Okazaki, A. T., Kato, S., & Fukue, J. 1987, PASJ, 39, 457
Ortega-Rodriguez, M., & Wagoner, R. V. 2000, ApJ, in press (astro-ph/0002419)
Osaki, Y. 1985, A&A, 144, 369
Osaki, Y. 1996, PASP, 108, 39
Osaki, Y., Hirose, M., & Ichikawa, S. 1993, in Accretion Disks in Compact Stellar Systems, ed. J. C. Wheeler (Singapore: World Scientific), 272
Paczyński, B., & Wiita, P. J. 1980, A&A, 88, 23
Papaloizou, J. C. B., & Pringle, J. E. 1983, MNRAS, 202, 1181
Papaloizou, J. C. B., & Pringle, J. E. 1985, MNRAS, 208, 721
Papaloizou, J. C. B., & Szuszkiewicz, E. 1994, MNRAS, 268, 29
Perez, C. A., Silbertgleit, A. S., Wagoner, R. V., & Lehr, D. E. 1997, ApJ, 476, 589
Popham, R., & Narayan, R. 1992, ApJ, 394, 255
Pringle, J. E. 1977, MNRAS, 178, 195
Pringle, J. E. 1996, MNRAS, 281, 357
Silbergleit, A. S., Wagoner, R. V., & Ortega-Rodriguez, M. 2000, ApJ, in press (astro-ph/0004114)
Unno, W., Osaki, Y., Ando, H., Saio, H., & Shibahashi, H. 1989, Nonradial Oscillations of Stars (Tokyo: University of Tokyo Press)
Vishniac, E. T., & Diamond, P. 1989, ApJ, 347, 435
Wagoner, R. V. 1999, Phys. Rep., 311, 259
Whitehurst, R. 1988, MNRAS, 232, 35
Yamasaki, T., & Kato, S. 1996, PASJ, 48, 99
Yamasaki, T., & Kato, S., & Mineshige, S. 1995, PASJ, 47, 59